IEEE Access
Multidisciplinary | Rapid Review | Open Access Journal

Received June 26, 2020, accepted July 8, 2020, date of publication July 14, 2020, date of current version July 30, 2020.

Digital Object Identifier 10.1109/ACCESS.2020.3009131

A New Frame Synchronization Algorithm for Linear Periodic Channels With Memory

OREN KOLAMAN, (Student Member, IEEE), AND RON DABORA, (Senior Member, IEEE)
Department of Electrical and Computer Engineering, Ben-Gurion University of the Negev, Be'er Sheva 8410501, Israel

Corresponding author: Ron Dabora (ron@ee.bgu.ac.il)

This work was supported in part by the Israel Science Foundation under Grant 1681/18, and in part by the Israel Ministry of Economy through the HERON-5G Consortium.

ABSTRACT Identifying the start time of a sequence of symbols received at the receiver, commonly referred to as *frame synchronization*, is a critical task for achieving good performance in digital communications systems employing time-multiplexed transmission. In this work we focus on *frame synchronization* for linear channels with memory, in which the channel impulse response is periodic and the additive Gaussian noise is correlated and cyclostationary. Such channels appear in many communications scenarios, including narrowband power line communications and interference-limited wireless communications. We derive frame synchronization algorithms based on simplifications of the optimal likelihood-ratio test, assuming the channel impulse response is unknown at the receiver, which is applicable to many practical scenarios. The computational complexity of each of the derived algorithms is characterized, and a procedure for selecting nearly optimal synchronization sequences is proposed. The algorithms derived in this work achieve better performance than the noncoherent correlation detector, and, in fact, facilitate a controlled tradeoff between complexity and performance.

INDEX TERMS Frame synchronization, cyclostationary signals, linear periodically time-varying channels, CMA equalizer, hypothesis testing, likelihood ratio test.

I. INTRODUCTION

In digital communications, blocks of information bits are mapped into sequences of symbols taken from a finite constellation set. The transmitter partitions the stream of symbols into frames of finite duration, which are then sent to a receiver through a channel. In order for the receiver to successfully recover the information bits from the received distorted and noisy version of the transmitted signal, the receiver must first identify the physical parameters of the transmitted signal; In particular it has to first identify the starting time of a received frame before any subsequent processing task is applied. The process of identifying the beginning of a received information frame within a measured incoming stream of samples at the receiver is called frame synchronization (FS) [1], [2]. As an example, in time division multiple access (TDMA) systems, FS identifies the boundaries between the multiplexed users [3]. In the current work, the received signal consists of a convolution between the transmitted signal and a periodic channel impulse response (CIR), which generalizes upon the common linear time-invariant (LTI) channel model. Then, an additive cyclostationary Gaussian noise (ACGN) process with a finite correlation length is summed with the output of the convolution to form the overall received signal. The ACGN model generalizes upon the common additive stationary Gaussian noise model. The channel model described above represents many communications scenarios, including narrowband (NB) power line communications (PLC) and interference-limited wireless communications [4, Sec. 5], [5], [6]. Instances of these scenarios include non-orthogonal multiple access (NOMA) [7], [8], full duplex communications, cognitive communications [9], digital subscriber line (DSL) communications [10], as well as additional communications mediums and paradigms, including the ''Internet of Things'' [11]. In [6], we considered the joint estimation of the carrier frequency offset and the channel impulse response for this channel model, and proposed a compressed-sensing based approximate joint maximum likelihood estimator for these quantities. In this paper we study FS for the above received signal model, using the pilot-assisted approach, in which the transmitted signal contains a specifically designed synchronization sequence which is embedded into the random data [1], [12]. Accordingly, the objective of the FS algorithm developed in this work

The associate editor coordinating the review of this manuscript and approving it for publication was Filbert Juwono.

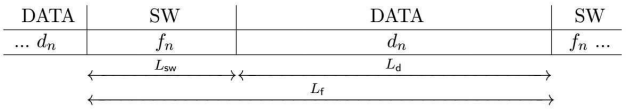

FIGURE 1. The structure of transmitted frame. Overall, the frame contains $L_f \in \mathcal{N}$ complex symbols and is divided into two parts: A synchronization word whose length is $L_{sw} \in \mathcal{N}$ and $L_d = (L_f - L_{sw})$ randomly selected data symbols denoted $\{d_n\}$.

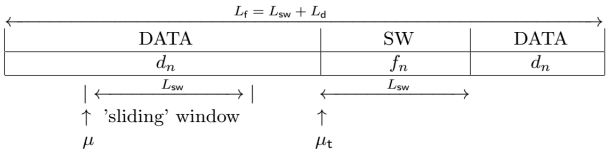

FIGURE 2. Frame synchronization process: μ_t is the true position of the synchronization sequence within the observation window and μ is the start position of the sliding search window within the received observation window.

is to identify the presence of the synchronization sequence within an observation window.

The common approach for frame synchronization is the *marker concept*, in which a known synchronization sequence, also referred as the synchronization word (SW), is incorporated into each transmitted data frame, as conceptually depicted in Fig 1. Assuming there is only one SW in each data frame, the synchronization algorithm observes the received signal and evaluates a mathematical function over a sliding search window whose duration is equal to the duration of the SW, as conceptually depicted in Fig. 2. There are two main detection approaches which utilize the marker concept: The first approach evaluates a test metric for all possible positions within the observation window and chooses the start position of the SW as the value of the start position which maximizes the test metric. This approach is referred to as one-shot point estimation (OSPE) FS, [13], [14]. The second approach compares the test metric computed for a specific start position within the observation window to a pre-determined threshold, such that once the threshold value is exceeded, the start position of the synchronization sequence is declared. Otherwise, the test metric is evaluated at the next position. This approach is commonly referred to as sequential FS [13], [14]. A study of the theoretical and implementation tradeoffs between OSPE FS and sequential FS for the general problem of FS in the presence of a large residual carrier frequency offset, is reported in [13]. OSPE FS algorithms for memoryless additive white Gaussian noise (AWGN) channels have been proposed in [12], [15]–[17], and for AWGN channels with memory in [18] and [19]. In [12], Massey showed that the optimal rule, in the sense of maximizing the probability of correctly locating the SW, for OSPE FS over memoryless AWGN channels with coherent binary phase-shift keying (BPSK) transmission is a correlator between the synchronization sequence and the received signal, modified by an additive correction term which is a function of the received signal. In [15], the performance of the optimal detector presented in [12] is analyzed, and an explicit expression for the probability of synchronization error, leading to incorrect SW start position estimation within the data frame, is derived. It is observed in [15] that the performance of the high SNR approximate optimal detector derived in [12], is practically indistinguishable from the performance of the optimal detector. The work [16] extended [12] to a general M-ary phase-coherent and phase-noncoherent signaling over AWGN channels. The work in [17] derived an OSPE FS algorithm for transmission of M-ary symbols over memoryless AWGN channels with unknown phase and frequency offsets. In [18], the work of [12] was extended to AWGN intersymbol interference (ISI) channels with BPSK transmission assuming the CIR is known at the receiver. In [19], an algorithm for OSPE FS over AWGN channels with ISI unknown at the receiver, and with an arbitrary symbol constellation, was presented. The work of [19] first estimates the unknown CIR via a maximum likelihood estimation assuming an arbitrary location for the SW. Then, the estimated CIR is plugged back into the likelihood function to obtain the likelihood value for the assumed location, thus facilitating a search for the maximizing value of the location. This scheme was next extended to handle also unknown CFO.

Sequential FS algorithms over memoryless AWGN channels have been proposed in [14], [20]–[24]. The work in [14] developed a sequential FS algorithm for BPSK transmission over memoryless AWGN channels with an unknown noise variance and an unknown channel gain. The work in [20] presented a sequential FS algorithm based on hypothesis testing, for pilot-symbol assisted modulation (PSAM) transmission [25], in which the pilot and the data symbols are selected from disjoint sets, and the signal is received over a memoryless AWGN channel such that the channel gain has an unknown random phase and frequency offsets. In [21], an hypothesis testing-based optimal FS algorithm for BPSK transmission over AWGN channels was proposed for detecting a SW. The work [21] assumed that the lengths of the frames are varying and are unknown at the receiver. The work in [22] extended the work of [21] to the case in which the probability distribution of the BPSK data symbols is unknown, which led to the derivation of a generalized likelihood ratio test (GLRT). In [24], a sequential FS algorithm was presented for BPSK transmission over memoryless AWGN channels, received with an unknown random carrier phase offset. To the best of our knowledge, a sequential FS algorithm for channels with memory in which the CIR is unknown has not yet been derived, and this is the contribution of the current work.

Main Contributions: In this work we derive a sequential FS algorithm for channels with linear, periodically time-varying CIR and with ACGN, based on the likelihood ratio test (LRT) metric. The unique aspects of our work are the general channel model for which the algorithm is derived, as well as the rigorous approach used in the derivation, in contrast to the ad-hoc methods used in previous works. Novelty follows as previous works did not explicitly account for the channel memory in the derivation of the detector, due to its associated computational complexity. Moreover, our derived algorithm does not assume

knowledge of the CIR coefficients. To the best of our knowledge, an FS algorithm for an unknown linear channel with memory and ACGN, derived based on the LRT has not been previously presented. Furthermore, the proposed algorithm includes approximations which facilitate a tradeoff between complexity and performance. The computational complexity of the proposed scheme is then explicitly derived. Lastly, we propose a statistics-based approach for constructing good SWs. We demonstrate the superiority of the proposed algorithm over the very common correlator detector in an extensive simulation study. It should be noted that in this work we do not consider designing new low-correlation sequences, since an important insight which arises from the simulations is that once the CIR has memory and the noise has correlation, then the low-correlation property becomes less relevant for frame synchronization performance. This point is clearly demonstrated by the numerical evaluations, which include an exhaustive search over all SWs, whose conclusion is that the good SWs for the considered channels have a relatively large correlation.

The rest of this paper is organized as follows: Section II presents the notations and a brief background on cyclostationary random processes. Section III details the received signal model and the statement of the synchronization problem in the context of the model. Next, Section IV derives the exact LRT assuming known CIR, subsequently, Section VI presents complexity reduction of the exact LRT assuming channel knowledge, and Section V presents our main result, which is the derivation of a low-complexity synchronization algorithm for unknown CIR, along with its computational complexity. Lastly, Section VII presents the simulation results and discussion, and Section VIII presents some concluding remarks.

II. PRELIMINARIES AND BACKGROUND

A. NOTATIONS

We use upper-case letters, e.g., X, to denote random variables (RVs), lower-case letters, e.g., x, to denote deterministic values (including realizations of random variables), and calligraphic letters, e.g., $\mathcal{X}$, to denote sets. An exception to this rule are the deterministic constants $K, M, N, N_0, T_0, P_{\mathsf{h}}, P_{\mathsf{z}}, L_{\mathsf{sw}}, L_{\mathsf{f}}, L_{\mathsf{ch}}, L_{\mathsf{z}}, L_{\mathsf{h}}, L_{\mathsf{tot}}, L_{\mathsf{est}}, L_{\mathsf{EQ}}$, L_{d}, and N_{s}, which are defined explicitly as appropriate. Column vectors are denoted with boldface letters, e.g., $\mathbf{x}$ denotes a deterministic vector and $\mathbf{X}$ denotes a random vector. We use upper-case double-stroke letters to denote matrices, e.g., $\mathbb{A}$; the element at the i-th row and the l-th column of $\mathbb{A}$ is denoted with $[\mathbb{A}]_{i,l}$. $\mathbb{O}_{N\times M}$ and $\mathbb{I}_{N\times M}$ denote an $N \times M$ matrix of zeros, and an $N \times M$ matrix whose diagonal elements are all 1 and all off-diagonal elements are zero, respectively. $\mathcal{C}$, $\mathcal{R}$, $\mathcal{N}$, and $\mathcal{Z}$ denote the sets of complex numbers, real numbers, natural numbers, and integers, respectively. Complex conjugate, transpose, Hermitian transpose, Euclidean norm, and stochastic expectation, are denoted by $(\cdot)^*$, $(\cdot)^T$, $(\cdot)^H$, $\|\cdot\|$, $\mathbb{E}\{\cdot\}$. We use $|\cdot|$ to denote magnitude when applied to scalars, and the determinant when applied to matrices, and $\delta[\cdot]$ is used for denoting the Kronecker impulse function. We use j to denote the imaginary unit, that is $j^2 = -1$.

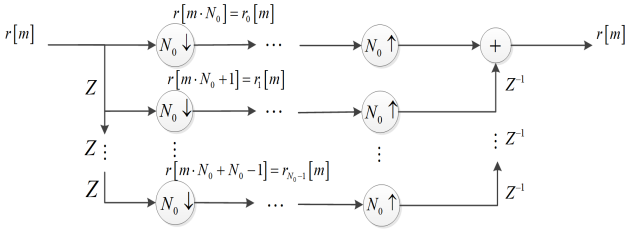

FIGURE 3. Schematic description of the decimated components decomposition.

B. CYCLOSTATIONARY STOCHASTIC PROCESSES

In the following we briefly overview some aspects of wide-sense cyclostationary (WSCS) random processes.

Definition 1: [4], [26] A discrete-time proper-complex stochastic process $R[n]$ is called a WSCS stochastic process, if its mean and its autocorrelation functions are periodic with period $N_0 \in \mathcal{N}$, that is:

$$\begin{aligned}\mathbb{E}\{R[m]\} &= \mathbb{E}\{R[m+N_0]\},\ m \in \mathcal{Z},\\ c_R[m,l] &\triangleq \mathbb{E}\{R[m+l]\cdot(R[m])^*\}\\ &= c_R[m+N_0,l],\quad m,l \in \mathcal{Z}.\end{aligned}$$

The corresponding definition for continuous-time (CT) processes simply replaces the time variable $m, l \in \mathcal{Z}$ with $t, \tau \in \mathcal{R}$ and the period $N_0 \in \mathcal{N}$ with $T_0 \in \mathcal{R}^{++}$. WSCS stochastic processes are encountered in many outcomes of man-made actions as well as in natural phenomena with periodic characteristics. Instances of cyclostationarity include communications [4, Clause 7.1], econometric modeling [27], atmospheric science [24], and biological systems [28]. A comprehensive overview of DT cyclostationary processes which are at the focus of this work is provided in [26].

The decimated components decomposition (DCD) is a mapping which transforms a complex scalar DT WSCS process $R[m]$ with period N_0 into an equivalent $N_0 \times 1$ multivariate wide-sense stationary (WSS) process $\mathbf{R}[n] \in \mathbb{C}^{N_0\times 1}$ [4, Clause 3.10], [26], defined as:

$$\mathbf{R}[n] = \begin{pmatrix} R_0[n]\\ R_1[n]\\ \vdots\\ R_{N_0-1}[n]\end{pmatrix},\ \big[\mathbf{R}[n]\big]_q = R_q[n] \triangleq R[nN_0-q],$$
$$n \in \mathbb{Z},\ N_0 \in \mathcal{N},\ q = 0,1,\ldots,N_0-1.$$

This transformation is schematically described in Fig. 3. Letting $0 \le a_1, a_2 \le N_0-1$ the auto-correlation matrix of $\mathbf{R}[n]$, defined as $\mathbb{R}_{\mathbf{R}}[n,l] \triangleq \mathbb{E}\{\mathbf{R}[n+l](\mathbf{R}[n])^H\}$ is obtained as:

$$\begin{aligned}&\big[\mathbb{R}_{\mathbf{R}}[n,l]\big]_{a_1+1,a_2+1}\\ &= \mathbb{E}\{R[(n+l)N_0-a_1]\cdot(R[nN_0-a_2])^*\}\\ &= c_R[nN_0-a_2, lN_0+a_2-a_1]\\ &\overset{(a)}{=} c_R[-a_2, lN_0+a_2-a_1]\end{aligned}$$

where (a) follows from the fact that $R[n]$ is a WSCS stochastic process with period N_0. Observe that $\mathbb{R}_{\mathbf{R}}[n,l] = \mathbb{R}_{\mathbf{R}}[l] \in \mathcal{C}^{N_0 \times N_0}$ which is independent of n. It is also straightforward to verify that $\mathbb{E}\{\mathbf{R}[n]\}$ is a constant vector, implying that $\mathbf{R}[n]$ is WSS. The cyclostationary process $R[m]$ can be recovered from the vector process $\mathbf{R}[n]$ via:

$$R[m] = \sum_{i=0}^{N_0-1} \sum_{l=-\infty}^{\infty} \big[\mathbf{R}[l]\big]_i \cdot \delta[m - i - lN_0],$$

as depicted in Figure 3.

III. SIGNAL MODEL AND PROBLEM FORMULATION

In this section we first introduce the models for the DT transmitted signal and for the corresponding received signal, and then formulate the frame synchronization problem as a hypothesis testing problem.

A. RECEIVED SIGNAL MODEL

We consider communications over an additive noise channel with a linear periodically time-varying (LPTV) CIR, denoted with $h[m,l]$, such that when the channel input is $\delta[m-l_0]$, $m, l_0 \in \mathcal{Z}$, i.e., an impulse which is introduced at the input of the channel at time l_0, the output is $h[m, m-l_0]$. We let $P_{\mathsf{h}} \in \mathcal{N}$ denote the periodicity of the CIR, i.e.,

$$h[m + P_{\mathsf{h}}, l] = h[m,l], \quad m, l \in \mathcal{Z}.$$

We observe that when $P_{\mathsf{h}} = 1$, then the periodic CIR $h[m,l]$ specializes to an LTI CIR, as for any $m \in \mathcal{Z}$ it follows that $h[m,l] = h[0,l]$, and we may thus denote $h[0,l] \equiv h[l]$. The communications channel is assumed to be casual with a finite memory, and a maximal length denoted by $L_{\mathsf{h}} \in \mathcal{N}$:

$$\exists m_1 \in \mathcal{Z} \text{ s.t. } h[m_1, 0] \neq 0,\ \exists m_2 \in \mathcal{Z} \text{ s.t. } h[m_2, L_{\mathsf{h}}] \neq 0,$$
$$\text{and } h[m,l] = 0,\ \forall\, l < 0 \text{ and } \forall\, l > L_{\mathsf{h}},\ \forall\, m \in \mathcal{Z}.$$

The received signal is contaminated by an ACGN[1] process $Z[m]$, which is a zero-mean, baseband, proper complex process. The process $Z[m]$ has a period of $P_{\mathsf{z}} \in \mathcal{N}$ and a finite correlation memory of $L_{\mathsf{z}} \in \mathcal{N}$:

$$\mathbb{E}\{Z[m]\} = 0 \tag{1a}$$
$$c_{\mathsf{z}}[m,l] \triangleq \mathbb{E}\Big\{Z[m+l] \cdot \big(Z[m]\big)^*\Big\} = c_{\mathsf{z}}[m + P_{\mathsf{z}}, l] \tag{1b}$$
$$c_{\mathsf{z}}[m,l] = 0 \ \text{ for } |l| > L_{\mathsf{z}}, \quad \forall\, m \in \mathcal{Z}\,, \tag{1c}$$

where $c_{\mathsf{z}}[m,l]$ *is assumed known at the receiver.* We observe that with $P_{\mathsf{z}} = 1$ the periodic autocorrlation function $c_{\mathsf{z}}[m,l]$ specializes to a time-invariant autocorrelation function $c_{\mathsf{z}}[l]$, corresponding to a WSS random noise process. The symbol sequence $S[m]$ is an independent and identically distributed (i.i.d) sequence of complex symbols, selected from a finite constellation set $\mathcal{S} = \{s_0, s_1, \ldots, s_{N_{\mathsf{s}}-1}\}$, such that $s_i \in \mathcal{C}$, $i = 0, 1, \ldots, N_{\mathsf{s}}-1$, according to a uniform distribution, with the first and second moments given by:

$$\mathbb{E}\{S[m]\} = 0, \quad \forall\, m \in \mathcal{Z}. \tag{2a}$$
$$\mathbb{E}\Big\{S[m_1] \cdot \big(S[m_2]\big)^*\Big\} = \sigma_{\mathsf{s}}^2 \cdot \delta[m_1 - m_2], \quad \sigma_{\mathsf{s}}^2 \in \mathcal{R}^{++},\ \forall\, m_1, m_2 \in \mathcal{Z}. \tag{2b}$$
$$\mathbb{E}\Big\{S[m_1] \cdot S[m_2]\Big\} = \tilde{\sigma}_{\mathsf{s}}^2 \cdot \delta[m_1 - m_2], \quad \tilde{\sigma}_{\mathsf{s}}^2 \in \mathcal{C}, \quad \forall\, m_1, m_2 \in \mathcal{Z}. \tag{2c}$$

Eq. (2c) characterizes the pseudo-covariance of the symbol sequence $S[m]$. The symbol and noise processes, $S[m]$ and $Z[m]$, are mutually independent.

Letting, let $L_{\mathsf{ch}} \triangleq \max\{L_{\mathsf{z}}, L_{\mathsf{h}}\}$ denote the memory of the channel, we express the relationship between the realizations of the DT received signal $R[m]$, the transmitted symbol process $S[m]$ and the noise process $Z[m]$ as:

$$r[m] = \sum_{l=0}^{L_{\mathsf{ch}}} h[m,l]s[m-l] + z[m], \quad m \in \mathcal{Z}. \tag{3}$$

This model is a generalization of the LTI channel with additive WSS noise. It is assumed that $h[m,l]$ is deterministic and unknown except for its period P_{h} and memory length L_{ch}, and that the values of the coefficients $h[m,l]$ remain the same throughout the frame synchronization process. A signal frame consists of $L_{\mathsf{f}} \in \mathcal{N}$ complex symbols and is conceptually divided into two parts as depicted in Figure 1: One part is an SW, which consists of $L_{\mathsf{sw}} \in \mathcal{N}$ complex symbols $\mathbf{f}_{\mathsf{sw}}^T = [f_{L_{\mathsf{sw}}-1}, f_{L_{\mathsf{sw}}-2}, \ldots, f_0]$, where $L_{\mathsf{sw}} \ll L_{\mathsf{f}}$. The second part is $L_{\mathsf{d}} = (L_{\mathsf{f}} - L_{\mathsf{sw}})$ randomly selected data symbols denoted $\{d_n\}$. Letting N be a multiple of the least common multiple (LCM) of the discrete periods P_{h} and P_{z} that satisfies $N > L_{\mathsf{ch}}$, it follows that there exist $k_1, k_2 \in \mathcal{N}$ s.t. $k_1 P_{\mathsf{h}} = k_2 P_{\mathsf{z}} = N$. The length of the synchronization sequence, L_{sw}, is set to satisfy $L_{\mathsf{sw}} > L_{\mathsf{ch}} + 1$. Upon transmission, the transmitter applies the following preprocessing: The SW of L_{sw} complex symbols is divided into $M \in \mathcal{N}$ blocks, each containing $K \triangleq (N - L_{\mathsf{ch}})$ complex symbols, such that $L_{\mathsf{sw}} = KM$. With this partition, we can write $\mathbf{f}_{\mathsf{sw}}^T = [\mathbf{t}_{M-1}^T, \mathbf{t}_{M-2}^T, \ldots, \mathbf{t}_0^T]$, where $\mathbf{t}_i = [f_{iK+K-1}, f_{iK+K-2}, \ldots, f_{iK}]^T$, $i = 0, 1, \ldots, M-1$. At the end of each $\mathbf{t}_i$ block of length K, the transmitter inserts L_{ch} data symbols[2] as depicted in Figure 4, such that the total length of the sequence transmitted for synchronization is $L_{\mathsf{tot}} \triangleq L_{\mathsf{sw}} + ML_{\mathsf{ch}} = KM + ML_{\mathsf{ch}} = (N - L_{\mathsf{ch}}) \cdot M + ML_{\mathsf{ch}} = NM$, where it is assumed that $L_{\mathsf{tot}} \ll L_{\mathsf{f}}$. The objective of the synchronization detector is to identify the beginning of a frame by observing L_{tot} subsequent samples collected from the received signal, stated as:

$$r[m-i] = \sum_{l=0}^{L_{\mathsf{ch}}} h[m-i, l]s[m-i-l] + z[m-i], \quad i = 0, 1, \ldots, L_{\mathsf{tot}} - 1$$

[1] In [29, Appendix A] it is shown that under rather general conditions it follows that the baseband representation of a real bandlimited passband WSCS Gaussian channel is a proper complex WSCS Gaussian process.

[2] It is possible to add a guard interval instead of data symbols if so desired, yet using data symbols will result in a higher spectral efficiency.

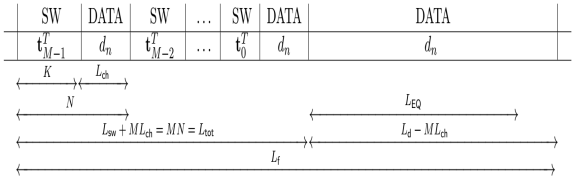

FIGURE 4. Structure of a transmitted frame containing SW and random data.

B. STATEMENT OF THE HYPOTHESIS TESTING PROBLEM

We begin by defining the quantities to be used in the derivations of the algorithm. We use the column vector notation $\mathbf{x}_{T_\mathsf{x},d_\mathsf{x}}[n] \in \mathcal{C}^{L_\mathsf{x}\times 1}$ with constants T_x, $L_\mathsf{x} \in \mathcal{N}$, $d_\mathsf{x} \in \{0,1,\ldots T_\mathsf{x}-1\} \triangleq \mathcal{T}_\mathsf{x}$, defined as:

$$\mathbf{x}_{T_\mathsf{x},d_\mathsf{x}}[n] \triangleq \begin{pmatrix} x\big[n\cdot T_\mathsf{x} - d_\mathsf{x}\big] \\ x\big[n\cdot T_\mathsf{x} - d_\mathsf{x} - 1\big] \\ \vdots \\ x\big[n\cdot T_\mathsf{x} - d_\mathsf{x} - (L_\mathsf{x}-1)\big] \end{pmatrix}, \quad 0 \le d_x \le T_\mathsf{x} - 1.$$

With this notation, we express the received vector $\mathbf{r}_{L_\mathsf{tot},d_\mathsf{r}}[n] \in \mathcal{C}^{L_\mathsf{tot}\times 1}$ of L_tot subsequent samples as:

$$\mathbf{r}_{L_\mathsf{tot},d_\mathsf{r}}[n] \triangleq \begin{pmatrix} r\big[n\cdot L_\mathsf{tot} - d_\mathsf{r}\big] \\ r\big[n\cdot L_\mathsf{tot} - d_\mathsf{r} - 1\big] \\ \vdots \\ r\big[n\cdot L_\mathsf{tot} - d_\mathsf{r} - (L_\mathsf{tot}-1)\big] \end{pmatrix}, \quad 0 \le d_r \le L_\mathsf{tot} - 1. \tag{4}$$

Choosing proper values for d_r and n, allows us to collect different L_tot subsequent samples from the received signal frame. Next, we define the notation $h^{(d_\mathsf{r})}_{n,k,l} \triangleq h\big[n\cdot L_\mathsf{tot} - d_\mathsf{r} - k, l\big]$, $k = 0,1,\ldots,L_\mathsf{tot}-1$ and express $\mathbf{r}_{L_\mathsf{tot},d_\mathsf{r}}[n]$ in a matrix form using the following matrices and vectors:

$$\mathbf{s}^{(m)}_{L_\mathsf{tot},d_\mathsf{r}}[n] \triangleq \begin{pmatrix} s\big[n\cdot L_\mathsf{tot} - m\cdot N - d_\mathsf{r}\big] \\ s\big[n\cdot L_\mathsf{tot} - m\cdot N - d_\mathsf{r} - 1\big] \\ \vdots \\ s\big[n\cdot L_\mathsf{tot} - m\cdot N - d_\mathsf{r} - (K-1)\big] \end{pmatrix},$$

$$\mathbf{d}^{(m)}_{L_\mathsf{tot},d_\mathsf{r}}[n] \triangleq \begin{pmatrix} s\big[n\cdot L_\mathsf{tot} - m\cdot N - d_\mathsf{r} - K\big] \\ s\big[n\cdot L_\mathsf{tot} - m\cdot N - d_\mathsf{r} - (K+1)\big] \\ \vdots \\ s\big[n\cdot L_\mathsf{tot} - m\cdot N - d_\mathsf{r} - (N-1)\big] \end{pmatrix},$$

$$m = 0,1,\ldots,M-1$$
$$\mathbf{s}^{(m)}_{L_\mathsf{tot},d_\mathsf{r}}[n] \in \mathcal{C}^{K\times 1},\ \mathbf{d}^{(m)}_{L_\mathsf{tot},d_\mathsf{r}}[n] \in \mathcal{C}^{(N-K)\times 1}$$

and for transmission block m we write

$$\mathbf{g}^{(m)}_{L_\mathsf{tot},d_\mathsf{r}}[n] \triangleq \begin{pmatrix} \mathbf{s}^{(m)}_{L_\mathsf{tot},d_\mathsf{r}}[n] \\ \mathbf{d}^{(m)}_{L_\mathsf{tot},d_\mathsf{r}}[n] \end{pmatrix} \in \mathcal{C}^{N\times 1}, \quad m = 0,1,\ldots,M-1. \tag{5}$$

Lastly, define:

$$\mathbf{l}_{L_\mathsf{tot},d_\mathsf{r}}[n] \triangleq \begin{pmatrix} s\big[n\cdot L_\mathsf{tot} - M\cdot N - d_\mathsf{r}\big] \\ s\big[n\cdot L_\mathsf{tot} - M\cdot N - d_\mathsf{r} - 1\big] \\ \vdots \\ s\big[n\cdot L_\mathsf{tot} - M\cdot N - d_\mathsf{r} - (L_\mathsf{ch}-1)\big] \end{pmatrix}, \quad \mathbf{l}_{L_\mathsf{tot},d_\mathsf{r}}[n] \in \mathcal{C}^{L_\mathsf{ch}\times 1}.$$

Each vector $\mathbf{s}^{(m)}_{L_\mathsf{tot},d_\mathsf{r}}[n]$ consists of only random data symbols when the synchronization word is outside the observation window and of the SW symbols when the synchronization word is within the observation window. The vectors $\mathbf{d}^{(m)}_{L_\mathsf{tot},d_\mathsf{r}}[n]$ and $\mathbf{l}_{L_\mathsf{tot},d_\mathsf{r}}[n]$ consist of only random data symbols. With these definitions we can express the overall signal used for generating the observed samples as:

$$\mathbf{s}_{L_\mathsf{tot},d_\mathsf{r}}[n] \triangleq \begin{pmatrix} \mathbf{g}^{(0)}_{L_\mathsf{tot},d_\mathsf{r}}[n] \\ \mathbf{g}^{(1)}_{L_\mathsf{tot},d_\mathsf{r}}[n] \\ \vdots \\ \mathbf{g}^{(M-1)}_{L_\mathsf{tot},d_\mathsf{r}}[n] \\ \mathbf{l}_{L_\mathsf{tot},d_\mathsf{r}}[n] \end{pmatrix} = \begin{pmatrix} \mathbf{s}^{(0)}_{L_\mathsf{tot},d_\mathsf{r}}[n] \\ \mathbf{d}^{(0)}_{L_\mathsf{tot},d_\mathsf{r}}[n] \\ \mathbf{s}^{(1)}_{L_\mathsf{tot},d_\mathsf{r}}[n] \\ \mathbf{d}^{(1)}_{L_\mathsf{tot},d_\mathsf{r}}[n] \\ \vdots \\ \mathbf{s}^{(M-1)}_{L_\mathsf{tot},d_\mathsf{r}}[n] \\ \mathbf{d}^{(M-1)}_{L_\mathsf{tot},d_\mathsf{r}}[n] \\ \mathbf{l}_{L_\mathsf{tot},d_\mathsf{r}}[n] \end{pmatrix},$$
$$\mathbf{s}_{L_\mathsf{tot},d_\mathsf{r}}[n] \in \mathcal{C}^{(L_\mathsf{tot}+L_\mathsf{ch})\times 1},$$

and the respective noise component as

$$\mathbf{z}_{L_\mathsf{tot},d_\mathsf{r}}[n] \triangleq \begin{pmatrix} z\big[n\cdot L_\mathsf{tot} - d_\mathsf{r}\big] \\ z\big[n\cdot L_\mathsf{tot} - d_\mathsf{r} - 1\big] \\ \vdots \\ z\big[n\cdot L_\mathsf{tot} - d_\mathsf{r} - (L_\mathsf{tot}-1)\big] \end{pmatrix}, \quad \mathbf{z}_{L_\mathsf{tot},d_\mathsf{r}}[n] \in \mathcal{C}^{L_\mathsf{tot}\times 1}. \tag{6}$$

Lastly, we define the matrix $\mathbb{A}_{L_\mathsf{tot},d_\mathsf{r}}[n] \in \mathcal{C}^{L_\mathsf{tot}\times(L_\mathsf{tot}+L_\mathsf{ch})}$:

$$\mathbb{A}_{L_\mathsf{tot},d_\mathsf{r}}[n] \triangleq \begin{pmatrix} h^{(d_\mathsf{r})}_{n,0,0} & h^{(d_\mathsf{r})}_{n,0,1} & h^{(d_\mathsf{r})}_{n,0,2} & \cdots & h^{(d_\mathsf{r})}_{n,0,L_\mathsf{ch}} & 0 & \cdots & 0 \\ 0 & h^{(d_\mathsf{r})}_{n,1,0} & h^{(d_\mathsf{r})}_{n,1,1} & \cdots & h^{(d_\mathsf{r})}_{n,1,L_\mathsf{ch}-1} & h^{(d_\mathsf{r})}_{n,1,L_\mathsf{ch}} & \cdots & 0 \\ 0 & 0 & h^{(d_\mathsf{r})}_{n,2,0} & \cdots & h^{(d_\mathsf{r})}_{n,2,L_\mathsf{ch}-2} & h_{n,2,L_\mathsf{ch}-1} & h^{(d_\mathsf{r})}_{n,2,L_\mathsf{ch}} & \cdots \\ \vdots & \vdots & \vdots & \ddots & \vdots & \vdots & \vdots & \ddots \\ 0 & 0 & 0 & \cdots & 0 & 0 & 0 & \cdots \end{pmatrix}. \tag{7}$$

Using the definitions above, the relationship between the signal received within the observation window and the transmitted signal can be expressed in a vector form as:

$$\mathbf{r}_{L_{\text{tot}},d_{\text{r}}}[n] = \mathbb{A}_{L_{\text{tot}},d_{\text{r}}}[n] \cdot \mathbf{s}_{L_{\text{tot}},d_{\text{r}}}[n] + \mathbf{z}_{L_{\text{tot}},d_{\text{r}}}[n], \quad n \in \mathcal{Z}. \tag{8}$$

At the receiver, the received vector signal $\mathbf{r}_{L_{\text{tot}},d_{\text{r}}}[n]$ is applied post-processing, denoted $\mathsf{P}\{\mathbf{r}_{L_{\text{tot}},d_{\text{r}}}[n]\}$, designed to extract only the relevant information for synchronization as follows: The received vector $\mathbf{r}_{L_{\text{tot}},d_{\text{r}}}[n]$ is first divided into M component vectors of length N. Then, for each component vector, the last L_{ch} samples are discarded resulting in the following processed vector:

$$\mathsf{P}\{\mathbf{r}_{L_{\text{tot}},d_{\text{r}}}[n]\} \equiv \mathbf{r}^{(\mathsf{P})}_{L_{\text{tot}},d_{\text{r}}}[n] \triangleq \begin{pmatrix} \tilde{\mathbf{r}}_{N,d_{\text{r}}}[n\cdot M] \\ \tilde{\mathbf{r}}_{N,d_{\text{r}}}[n\cdot M-1] \\ \vdots \\ \tilde{\mathbf{r}}_{N,d_{\text{r}}}[n\cdot M-(M-1)] \end{pmatrix},$$

$$\tilde{\mathbf{r}}_{N,d_{\text{r}}}[n] \triangleq \begin{pmatrix} r[n\cdot N-d_{\text{r}}] \\ r[n\cdot N-d_{\text{r}}-1] \\ \vdots \\ r[n\cdot N-d_{\text{r}}-(K-1)] \end{pmatrix},$$

$$\mathbf{r}^{(\mathsf{P})}_{L_{\text{tot}},d_{\text{r}}}[n] \in \mathcal{C}^{L_{\text{sw}}\times 1},\ \tilde{\mathbf{r}}_{N,d_{\text{r}}}[n] \in \mathcal{C}^{K\times 1}. \tag{9}$$

Next, for $l = 0,1,\ldots,K-1$, $m = 0,1,\ldots,M-1$ and $k = 0,1,\ldots,L_{\text{tot}}-1$, we define the following matrices and vectors:

$$\mathbf{h}^{(d_{\text{r}},l)}[n,k] \triangleq \begin{pmatrix} \mathbb{O}_{l\times 1} \\ \tilde{\mathbf{h}}^{(d_{\text{r}})}[n,k] \\ \mathbb{O}_{(N-l-L_{\text{ch}}-1)\times 1} \end{pmatrix} \in \mathcal{C}^{N\times 1}$$

$$\tilde{\mathbf{h}}^{(d_{\text{r}})}[n,k] \triangleq \begin{pmatrix} h^{(d_{\text{r}})}_{n,k,0} \\ h^{(d_{\text{r}})}_{n,k,1} \\ \vdots \\ h^{(d_{\text{r}})}_{n,k,L_{\text{ch}}} \end{pmatrix} \in \mathcal{C}^{(L_{\text{ch}}+1)\times 1}$$

$$\mathbb{B}^{(d_{\text{r}},m)}[n] \triangleq \begin{pmatrix} \left(\mathbf{h}^{(d_{\text{r}},0)}[n,m\cdot N]\right)^T \\ \left(\mathbf{h}^{(d_{\text{r}},1)}[n,m\cdot N+1]\right)^T \\ \vdots \\ \left(\mathbf{h}^{(d_{\text{r}},K-1)}[n,m\cdot N+K-1]\right)^T \end{pmatrix},$$

$$\mathbb{B}^{(d_{\text{r}},m)}[n] \in \mathcal{C}^{K\times N}. \tag{10}$$

We also define

$$\mathbb{A}^{(\mathsf{P})}_{L_{\text{tot}},d_{\text{r}}}[n] \triangleq \begin{pmatrix} \mathbb{B}^{(d_{\text{r}},0)}[n] & \mathbb{O}_{K\times N} & \ldots & \mathbb{O}_{K\times N} \\ \mathbb{O}_{K\times N} & \mathbb{B}^{(d_{\text{r}},1)}[n] & \ldots & \mathbb{O}_{K\times N} \\ \mathbb{O}_{K\times N} & \mathbb{O}_{K\times N} & \ldots & \mathbb{O}_{K\times N} \\ \vdots & \vdots & \ddots & \vdots \\ \mathbb{O}_{K\times N} & \mathbb{O}_{K\times N} & \ldots & \mathbb{B}^{(d_{\text{r}},M-1)}[n] \end{pmatrix},$$

$$\mathbb{A}^{(\mathsf{P})}_{L_{\text{tot}},d_{\text{r}}}[n] \in \mathcal{C}^{L_{\text{sw}}\times L_{\text{tot}}}$$

$$\tilde{\mathbf{s}}_{L_{\text{tot}},d_{\text{r}}}[n] \triangleq \begin{pmatrix} \mathbf{s}^{(0)}_{L_{\text{tot}},d_{\text{r}}}[n] \\ \mathbf{d}^{(0)}_{L_{\text{tot}},d_{\text{r}}}[n] \\ \mathbf{s}^{(1)}_{L_{\text{tot}},d_{\text{r}}}[n] \\ \vdots \\ \mathbf{s}^{(M-1)}_{L_{\text{tot}},d_{\text{r}}}[n] \\ \mathbf{d}^{(M-1)}_{L_{\text{tot}},d_{\text{r}}}[n] \end{pmatrix} \in \mathcal{C}^{L_{\text{tot}}\times 1}$$

$$\tilde{\mathbf{z}}_{N,d_{\text{r}}}[n] \triangleq \begin{pmatrix} z[n\cdot N-d_{\text{r}}] \\ z[n\cdot N-d_{\text{r}}-1] \\ \vdots \\ z[n\cdot N-d_{\text{r}}-(K-1)] \end{pmatrix} \in \mathcal{C}^{K\times 1}$$

$$\mathbf{z}^{(\mathsf{P})}_{L_{\text{tot}},d_{\text{r}}}[n] \triangleq \begin{pmatrix} \tilde{\mathbf{z}}_{N,d_{\text{r}}}[n\cdot M] \\ \tilde{\mathbf{z}}_{N,d_{\text{r}}}[n\cdot M-1] \\ \vdots \\ \tilde{\mathbf{z}}_{N,d_{\text{r}}}[n\cdot M-(M-1)] \end{pmatrix} \in \mathcal{C}^{L_{\text{sw}}\times 1}. \tag{11}$$

Using the relationship in (8) and the above definitions, we obtain the following relationship for the post-processed received vector:

$$\mathbf{r}^{(\mathsf{P})}_{L_{\text{tot}},d_{\text{r}}}[n] = \mathbb{A}^{(\mathsf{P})}_{L_{\text{tot}},d_{\text{r}}}[n] \cdot \tilde{\mathbf{s}}_{L_{\text{tot}},d_{\text{r}}}[n] + \mathbf{z}^{(\mathsf{P})}_{L_{\text{tot}},d_{\text{r}}}[n].$$

Recalling that the channel period is N, it follows that $h^{(d_{\text{r}})}_{n,k,l} = h^{(d_{\text{r}})}_{n,k+N,l}$, hence we conclude that $\mathbb{B}^{(d_{\text{r}},0)}[n] = \mathbb{B}^{(d_{\text{r}},1)}[n] = \ldots = \mathbb{B}^{(d_{\text{r}},M-1)}[n]$, and use $\mathbb{B}^{(d_{\text{r}})}[n]$ to denote $\mathbb{B}^{(d_{\text{r}},m)}[n] = \mathbb{B}^{(d_{\text{r}})}[n]$, $m = 0,1,\ldots,M-1$. With these definitions we can represent the vectors $\tilde{\mathbf{r}}_{N,d_{\text{r}}}[n\cdot M-m]$, $m = 0,1,\ldots,M-1$, which correspond to the segments of $\mathbf{r}^{(\mathsf{P})}_{L_{\text{tot}},d_{\text{r}}}[n]$, as:

$$\tilde{\mathbf{r}}_{N,d_{\text{r}}}[n\cdot M-m] = \mathbb{B}^{(d_{\text{r}})}[n]\cdot \mathbf{g}^{(m)}_{L_{\text{tot}},d_{\text{r}}}[n] + \tilde{\mathbf{z}}_{N,d_{\text{r}}}[n\cdot M-m], \quad m = 0,1,\ldots,M-1\,. \tag{12}$$

It is clarified that the received samples which are discarded by the post-processing, are ignored only for the purpose of the frame synchronization algorithm. Naturally, these samples can be stored for processing by the decoder in the data recovery step once the frame synchronizer has detected the beginning of a frame. Next, recall the partition of the SW into M blocks, as defined in Section III-A:

$$\mathbf{f}_{\text{sw}} \triangleq \begin{pmatrix} f_{L_{\text{sw}}-1} \\ f_{L_{\text{sw}}-2} \\ \vdots \\ f_0 \end{pmatrix} = \begin{pmatrix} \mathbf{t}_{M-1} \\ \mathbf{t}_{M-2} \\ \vdots \\ \mathbf{t}_0 \end{pmatrix} \in \mathcal{C}^{L_{\text{sw}}\times 1}.$$

In the following, when $\tilde{\mathbf{s}}_{L_{\mathsf{tot}},d_{\mathsf{r}}}[n]$ contains the SW we denote it as $\tilde{\mathbf{s}}^{(\mathsf{sw})}_{L_{\mathsf{tot}},d_{\mathsf{r}}}[n]$, which is defined as:

$$\tilde{\mathbf{s}}^{(\mathsf{sw})}_{L_{\mathsf{tot}},d_{\mathsf{r}}}[n] \triangleq \begin{pmatrix} \tilde{\mathbf{g}}^{(0)}_{L_{\mathsf{tot}},d_{\mathsf{r}}}[n] \\ \tilde{\mathbf{g}}^{(1)}_{L_{\mathsf{tot}},d_{\mathsf{r}}}[n] \\ \vdots \\ \tilde{\mathbf{g}}^{(M-1)}_{L_{\mathsf{tot}},d_{\mathsf{r}}}[n] \end{pmatrix} \triangleq \begin{pmatrix} \mathbf{t}_{M-1} \\ \mathbf{d}^{(0)}_{L_{\mathsf{tot}},d_{\mathsf{r}}}[n] \\ \mathbf{t}_{M-2} \\ \mathbf{d}^{(1)}_{L_{\mathsf{tot}},d_{\mathsf{r}}}[n] \\ \vdots \\ \mathbf{d}^{(M-2)}_{L_{\mathsf{tot}},d_{\mathsf{r}}}[n] \\ \mathbf{t}_0 \\ \mathbf{d}^{(M-1)}_{L_{\mathsf{tot}},d_{\mathsf{r}}}[n] \end{pmatrix} \in \mathcal{C}^{L_{\mathsf{tot}} \times 1},$$

$$\tilde{\mathbf{g}}^{(m)}_{L_{\mathsf{tot}},d_{\mathsf{r}}}[n] \triangleq \begin{pmatrix} \mathbf{t}_{M-1-m} \\ \mathbf{d}^{(m)}_{L_{\mathsf{tot}},d_{\mathsf{r}}}[n] \end{pmatrix} \in \mathcal{C}^{N \times 1},\ m = 0, 1, \ldots, M-1. \tag{13}$$

When $\tilde{\mathbf{s}}_{L_{\mathsf{tot}},d_{\mathsf{r}}}[n]$ does not contain the synchronization sequence (namely, it contains only data), we denote it as $\tilde{\mathbf{s}}^{(\mathsf{data})}_{L_{\mathsf{tot}},d_{\mathsf{r}}}[n] \in \mathcal{C}^{L_{\mathsf{tot}} \times 1}$. In the following, to reduce notational clutter, we set $d_{\mathsf{r}} = 0$. The hypothesis testing problem with $d_{\mathsf{r}} = 0$ (it is emphasized that this only simplifies notations in the subsequent derivations) after the post-processing $\mathsf{P}\{\cdot\}$ can be written as:

$$H_0 : \mathbf{R}^{(\mathsf{P})}_{L_{\mathsf{tot}},0}[n] = \mathbb{A}^{(\mathsf{P})}_{L_{\mathsf{tot}},0}[n] \cdot \tilde{\mathbf{S}}^{(\mathsf{data})}_{L_{\mathsf{tot}},0}[n] + \mathbf{Z}^{(\mathsf{P})}_{L_{\mathsf{tot}},0}[n] \tag{14a}$$

$$H_1 : \mathbf{R}^{(\mathsf{P})}_{L_{\mathsf{tot}},0}[n] = \mathbb{A}^{(\mathsf{P})}_{L_{\mathsf{tot}},0}[n] \cdot \tilde{\mathbf{S}}^{(\mathsf{sw})}_{L_{\mathsf{tot}},0}[n] + \mathbf{Z}^{(\mathsf{P})}_{L_{\mathsf{tot}},0}[n] \tag{14b}$$

where, $\mathbb{B}^{(0)}[n] \equiv \mathbb{B}[n]$, $\mathbf{h}^{(0,m)}[n,k] \equiv \mathbf{h}^{(m)}[n,k]$, $\tilde{\mathbf{h}}^{(0)}[n,k] \equiv \tilde{\mathbf{h}}[n,k]$ and $h^{(0)}_{n,k,l} \equiv h_{n,k,l}$. Our objective is to derive an algorithm to decide between H_0 and H_1 such that for any given probability of false alarm the probability of detection is maximized. In the derivations and subsequent analysis which follows, we shall not consider in the hypothesis testing setup the mixed scenario in which the observation window contains data symbols and part of the SW symbols, since in such cases a properly designed synchronization sequence mimics random data [30].

IV. DERIVATION OF THE LRT FOR THE FRAME SYNCHRONIZATION PROBLEM

In this section we develop the LRT [31] for testing the hypothesis H_0 vs. hypothesis H_1, stated in (14).

A. STATISTICS OF THE RECEIVED SIGNAL FOR HYPOTHESIS H_0

It is straightforward to show that $\mathbb{E}\{\tilde{\mathbf{R}}_{N,0}[n]|H_0\} = \mathbf{0}$, see [29, Appendix B] for the details. In Appendix A we prove that $\tilde{\mathbf{R}}_{N,0}[n]$ defined in (9), subject to the H_0 hypothesis is a WSS multivariate random process, and that its correlation matrix, denoted $\mathbb{C}_{\tilde{\mathbf{R}}_{N,0}[n\cdot M-m]|\mathbf{g}^{(m)}_{L_{\mathsf{tot}},0}[n],H_0}$ is equal to $\mathbb{C}_{\mathbf{z}}$.

Next, for representing the PDF of $\mathbf{R}^{(\mathsf{P})}_{L_{\mathsf{tot}},0}[n]$ under the H_0 hypothesis we define the following vectors:

$$\mathbf{a}_l \triangleq \begin{pmatrix} s_{(m_{0,l} \bmod N_{\mathsf{s}})} \\ s_{(m_{1,l} \bmod N_{\mathsf{s}})} \\ \vdots \\ s_{(m_{N-1,l} \bmod N_{\mathsf{s}})} \end{pmatrix} \in \mathcal{C}^{N \times 1},$$

where $m_{d,l} = \left\lfloor \frac{l}{(N_{\mathsf{s}})^d} \right\rfloor$, $l = 0, 1, \ldots, (N_{\mathsf{s}})^N - 1$, $d = 0, 1, \ldots, N-1$, and s_i, $i = 0, 1, \ldots, N_{\mathsf{s}} - 1$ are the elements of the constellation set $\mathcal{S}$, $|\mathcal{S}| = N_{\mathsf{s}}$. The set $\{\mathbf{a}_l\}_{l=0}^{(N_{\mathsf{s}})^N-1}$ represents $(N_{\mathsf{s}})^N$ vectors of length N, each containing a different combination of N symbols from $\mathcal{S}$. The PDF of $\mathbf{R}^{(\mathsf{P})}_{L_{\mathsf{tot}},0}[n]$ under the H_0 hypothesis is expressed as:

$$\begin{aligned} & f\left(\mathbf{R}^{(\mathsf{P})}_{L_{\mathsf{tot}},0}[n] \middle| H_0\right) \\ & \overset{(a)}{=} \prod_{m=0}^{M-1} f\left(\tilde{\mathbf{R}}_{N,0}[n\cdot M - m] \middle| H_0\right) \\ & \overset{(b)}{=} \sum_{l=0}^{(N_{\mathsf{s}})^{MN}-1} \frac{1}{(N_{\mathsf{s}})^{MN}} \\ & \qquad \cdot \prod_{m=0}^{M-1} f\left(\tilde{\mathbf{R}}_{N,0}[n\cdot M - m] \middle| \mathbf{g}^{(m)}_{L_{\mathsf{tot}},0}[n] = \mathbf{a}_{q_{(l,m)}},\ H_0\right) \\ & \overset{(c)}{=} \frac{1}{\left(N_{\mathsf{s}}\right)^{L_{\mathsf{tot}}} \cdot \left(\pi^K \cdot |\mathbb{C}_{\mathbf{z}}|\right)^M} \\ & \qquad \cdot \sum_{l=0}^{(N_{\mathsf{s}})^{L_{\mathsf{tot}}}-1} \exp\Bigg(-\sum_{m=0}^{M-1} \Big(\big(\tilde{\mathbf{r}}_{N,0}[n\cdot M - m] \\ & \qquad\qquad - \mathbb{B}[n] \cdot \mathbf{a}_{q_{(l,m)}}\big)^H \cdot \mathbb{C}_{\mathbf{z}}^{-1} \\ & \qquad\qquad \cdot \big(\tilde{\mathbf{r}}_{N,0}[n\cdot M - m] - \mathbb{B}[n] \cdot \mathbf{a}_{q_{(l,m)}}\big)\Big)\Bigg) \end{aligned}$$

where (a) follows from the discussion after Eq. (37), which establishes that subject to the H_0 hypothesis, the post-processing $\mathsf{P}\{\cdot\}$ results in mutually independent random vectors $\tilde{\mathbf{R}}_{N,0}[n\cdot M - m]$, $m \in \mathcal{M}$, (b) follows from the law of total probability [32, Ch. 4.7], where $q_{(l,m)} = \left(\left\lfloor \frac{l}{(N_{\mathsf{s}})^{mN}} \right\rfloor \bmod (N_{\mathsf{s}})^N\right)$, (c) follows form (12) which implies that $f\left(\tilde{\mathbf{R}}_{N,0}[n\cdot M-m] \middle| \mathbf{g}^{(m)}_{L_{\mathsf{tot}},0}[n] = \mathbf{a}_l,\ H_0\right) = f_{\tilde{\mathbf{Z}}_{N,0}}\left(\tilde{\mathbf{r}}_{N,0}[n\cdot M - m] - \mathbb{B}[n]\cdot\mathbf{a}_l\right)$, where $\tilde{\mathbf{Z}}_{N,0}[n\cdot M - m]$ has a Gaussian PDF, and we also applied $L_{\mathsf{tot}} = MN$.

B. STATISTICS OF THE RECEIVED SIGNAL FOR HYPOTHESIS H_1

We next characterize the statistics of $\tilde{\mathbf{R}}_{N,0}[n]$ subject to the H_1 hypothesis, and prove that $\tilde{\mathbf{R}}_{N,0}[n\cdot M - m]$, $m = 0, 1, \ldots, M-1$, subject to the H_1 hypothesis, are mutually independent (but not i.i.d). First, in Appendix B1 we show that the vectors $\tilde{\mathbf{R}}_{N,0}[n\cdot M - m]$, subject to the H_1 hypothesis, are mutually independent w.r.t. n and m, for

$m = 0, 1, \ldots, M-1$. Next, in Appendix B2 we show that the covariance matrix of $\tilde{\mathbf{R}}_{N,0}[n \cdot M - m]$, $m = 0, 1, \ldots, M-1$, subject to the H_1 hypothesis, and given $\tilde{\mathbf{g}}^{(m)}_{L_{\mathsf{tot}},0}[n]$, is equal to $\mathbb{C}_{\mathbf{Z}}$ specified in (38), that is:

$$\begin{aligned}
&\mathbb{C}_{\tilde{\mathbf{R}}_{N,0}[\cdot n \cdot M - m] | \tilde{\mathbf{g}}^{(m)}_{L_{\mathsf{tot}},0}[n], H_1} \\
&\triangleq \mathbb{E}\left\{\tilde{\mathbf{R}}_{N,0}[n \cdot M - m] \cdot \left(\tilde{\mathbf{R}}_{N,0}[n \cdot M - m]\right)^H \middle| \tilde{\mathbf{g}}^{(m)}_{L_{\mathsf{tot}},0}[n], H_1\right\} \\
&\quad - \mathbb{E}\left\{\tilde{\mathbf{R}}_{N,0}[n \cdot M - m] \middle| \tilde{\mathbf{g}}^{(m)}_{L_{\mathsf{tot}},0}[n], H_1\right\} \\
&\qquad \cdot \mathbb{E}\left\{\left(\tilde{\mathbf{R}}_{N,0}[n \cdot M - m]\right)^H \middle| \tilde{\mathbf{g}}^{(m)}_{L_{\mathsf{tot}},0}[n], H_1\right\} \\
&= \mathbb{C}_{\mathbf{Z}}.
\end{aligned}$$

Next, for representing the PDF of $\mathbf{R}^{(\mathsf{P})}_{L_{\mathsf{tot}},0}[n]$ subject to the H_1 hypothesis, we define the following vectors:

$$\tilde{\mathbf{a}}_{l,k} \triangleq \begin{pmatrix} \mathbf{t}_{M-1-k} \\ s_{(m_0 \bmod N_{\mathsf{s}})} \\ s_{(m_1 \bmod N_{\mathsf{s}})} \\ \vdots \\ s_{(m_{L_{\mathsf{ch}}-1} \bmod N_{\mathsf{s}})} \end{pmatrix} \in \mathcal{C}^{N \times 1},$$

where $m_d = \left\lfloor \frac{l}{(N_{\mathsf{s}})^d} \right\rfloor$, $l = 0, 1, \ldots, (N_{\mathsf{s}})^{L_{\mathsf{ch}}} - 1$, $d = 0, 1, \ldots, L_{\mathsf{ch}} - 1$, $k = 0, 1, \ldots, M-1$, where s_i, for $i = 0, 1, \ldots, N_{\mathsf{s}} - 1$, are the elements of the constellation set $\mathcal{S}$, $|\mathcal{S}| = N_{\mathsf{s}}$. The set $\{\tilde{\mathbf{a}}_{l,k}\}_{l=0,k=0}^{(N_{\mathsf{s}})^{L_{\mathsf{ch}}}-1,M-1}$ represents $M \cdot (N_{\mathsf{s}})^{L_{\mathsf{ch}}}$ vectors of length N, each containing a different combination of L_{ch} symbols from $\mathcal{S}$, which appends a block of K SW symbols out of the L_{sw} complex SW symbols. The PDF of $\mathbf{R}^{(\mathsf{P})}_{L_{\mathsf{tot}},0}[n]$ under the H_1 hypothesis is expressed as:

$$\begin{aligned}
&f\left(\mathbf{R}^{(\mathsf{P})}_{L_{\mathsf{tot}},0}[n] \middle| H_1\right) \\
&\overset{(a)}{=} \prod_{m=0}^{M-1} f\left(\tilde{\mathbf{R}}_{N,0}[n \cdot M - m] \middle| H_1\right) \\
&\overset{(b)}{=} \sum_{u=0}^{(N_{\mathsf{s}})^{ML_{\mathsf{ch}}}-1} \prod_{m=0}^{M-1} \frac{1}{(N_{\mathsf{s}})^{L_{\mathsf{ch}}}} \\
&\qquad \cdot f\left(\tilde{\mathbf{R}}_{N,0}[n \cdot M - m] \middle| \tilde{\mathbf{g}}^{(m)}_{L_{\mathsf{tot}},0}[n] = \tilde{\mathbf{a}}_{\tilde{q}_{(u,m)},m}, H_1\right) \\
&\overset{(c)}{=} \frac{1}{(N_{\mathsf{s}})^{ML_{\mathsf{ch}}} \cdot \left(\pi^K \cdot |\mathbb{C}_{\mathbf{Z}}|\right)^M} \\
&\qquad \cdot \sum_{u=0}^{(N_{\mathsf{s}})^{ML_{\mathsf{ch}}}-1} \exp\Bigg(- \sum_{m=0}^{M-1} \Big(\big(\tilde{\mathbf{r}}_{N,0}[n \cdot M - m] \\
&\qquad\qquad - \mathbb{B}[n] \cdot \tilde{\mathbf{a}}_{\tilde{q}_{(u,m)},m}\big)^H \cdot \mathbb{C}_{\mathbf{Z}}^{-1} \\
&\qquad\qquad \cdot \big(\tilde{\mathbf{r}}_{N,0}[n \cdot M - m] - \mathbb{B}[n] \cdot \tilde{\mathbf{a}}_{\tilde{q}_{(u,m)},m}\big)\Big)\Bigg)
\end{aligned}$$

where (a) follows since after the post-processing $\mathsf{P}\{\cdot\}$ the vectors $\tilde{\mathbf{R}}_{N,0}[n \cdot M - m]$ are mutually independent (but not i.i.d), in (b) we set $\tilde{q}_{(u,m)} = \left(\left\lfloor \frac{u}{(N_{\mathsf{s}})^{mL_{\mathsf{ch}}}} \right\rfloor \bmod (N_{\mathsf{s}})^{L_{\mathsf{ch}}}\right)$, (c) follows since when $\tilde{\mathbf{g}}^{(m)}_{L_{\mathsf{tot}},0}[n]$ is given, then for H_1, $\tilde{\mathbf{R}}_{N,0}[n \cdot M - m] = \mathbb{B}[n] \cdot \tilde{\mathbf{g}}^{(m)}_{L_{\mathsf{tot}},0}[n] + \tilde{\mathbf{Z}}_{N,0}[n \cdot M - m]$, therefore

$$\begin{aligned}
&f\left(\tilde{\mathbf{R}}_{N,0}[n \cdot M - m] \middle| \tilde{\mathbf{g}}^{(m)}_{L_{\mathsf{tot}},0}[n] = \tilde{\mathbf{a}}_{u,m}, H_1\right) \\
&\qquad = f_{\tilde{\mathbf{Z}}_{N,0}}\left(\tilde{\mathbf{R}}_{N,0}[n \cdot M - m] - \mathbb{B}[n] \cdot \tilde{\mathbf{a}}_{u,m}\right)
\end{aligned}$$

and we use the fact that $\tilde{\mathbf{Z}}_{N,0}[n \cdot M - m]$ is distributed according to a Gaussian PDF.

C. THE LRT

Using the derived expressions for the statistics of the received signal subject to H_0 and to H_1, the LRT for the case of *known CIR* can be expressed as [31, Ch. 2.2.1]:

$$\mathrm{LRT}\left(\mathbf{R}^{(\mathsf{P})}_{L_{\mathsf{tot}},0}[n]\right) = \frac{f\left(\mathbf{R}^{(\mathsf{P})}_{L_{\mathsf{tot}},0}[n] \middle| H_0\right)}{f\left(\mathbf{R}^{(\mathsf{P})}_{L_{\mathsf{tot}},0}[n] \middle| H_1\right)}$$

Then, taking the natural logarithm of both sides we obtain the following expression for the exact LRT:

$$\log_e \left(\frac{\left(\sum_{l=0}^{(N_{\mathsf{s}})^{L_{\mathsf{tot}}}-1} \exp\left(- \sum_{m=0}^{M-1} \left(\left(\tilde{\mathbf{r}}_{N,0}[n \cdot M - m] - \mathbb{B}[n] \cdot \mathbf{a}_{q_{(l,m)}}\right)^H \cdot \mathbb{C}_{\mathbf{Z}}^{-1} \cdot \left(\tilde{\mathbf{r}}_{N,0}[n \cdot M - m] - \mathbb{B}[n] \cdot \mathbf{a}_{q_{(l,m)}}\right)\right)\right)\right)}{\left(\sum_{u=0}^{(N_{\mathsf{s}})^{ML_{\mathsf{ch}}}-1} \exp\left(- \sum_{m=0}^{M-1} \left(\left(\tilde{\mathbf{r}}_{N,0}[n \cdot M - m] - \mathbb{B}[n] \cdot \tilde{\mathbf{a}}_{\tilde{q}_{(u,m)},m}\right)^H \cdot \mathbb{C}_{\mathbf{Z}}^{-1} \cdot \left(\tilde{\mathbf{r}}_{N,0}[n \cdot M - m] - \mathbb{B}[n] \cdot \tilde{\mathbf{a}}_{\tilde{q}_{(u,m)},m}\right)\right)\right)\right)} \right) \underset{H_1}{\overset{H_0}{\gtrless}} \log_e\left(\lambda \cdot (N_{\mathsf{s}})^{MK}\right). \quad (15)$$

Computational Complexity: The computational complexity of the LRT was derived in terms of complex multiplications (CMs) and complex additions (CAs) in [29, Appendix D]. The total complexity of the LRT detector in Eq. (15) is:

$$\begin{aligned}
\mathrm{CM}(\mathrm{LRT}) &= MK \cdot (N + K + 1) \cdot \left((N_{\mathsf{s}})^{L_{\mathsf{tot}}} + (N_{\mathsf{s}})^{ML_{\mathsf{ch}}}\right) + 1 \\
\mathrm{CA}(\mathrm{LRT}) &= M \cdot \left(KN + (K-1) \cdot (K+1)\right) \cdot \left((N_{\mathsf{s}})^{L_{\mathsf{tot}}} + (N_{\mathsf{s}})^{ML_{\mathsf{ch}}}\right).
\end{aligned}$$

We observe that the expression (15) is very *intensive computationally* and it also requires *knowledge of the CIR coefficients*. In the next sections we apply approximations to obtain a computationally practical expression which does not require apriori knowledge of the CIR coefficients.

V. THE RALRT FRAME SYNCHRONIZATION ALGORITHM: REDUCING COMPLEXITY OF THE LRT

The main disadvantage of the optimal LRT in (15) is its high computational complexity which increases exponentially with the length of the SW. This follows as computation is carried out over $(N_{\mathsf{s}})^{L_{\mathsf{tot}}} - 1$ elements. In the following we reduce

the complexity of the LRT in two steps: First, we replace the summation over the exponents with the difference between two minimizations. We refer to the resulting detector as the approximate LRT (ALRT). Then, we propose a reduced complexity computation of the two minimizations, by reducing the search space for the minima. We refer to the resulting detection as the reduced approximate LRT (RALRT).

A. THE ALRT: APPROXIMATING THE LRT AS THE DIFFERENCE OF TWO MINIMA

We begin the approximation of the difference of the logarithms of sums of exponentials by recalling the following relationship for real numbers $\{x_l\}_{l=1}^{L}$ [33, Eq. (5)]:

$$\begin{aligned}\max\{x_1, x_2, \ldots, x_L\} &\le \log_e\left(\sum_{l=1}^{L} e^{x_l}\right)\\ &\le \max\{x_1, x_2, \ldots, x_L\} + \log_e(L)\,. \quad (16)\end{aligned}$$

Using (16) we can write the following inequality for two sequences $\{x_i\}_{i=1}^{L_0}$ and $\{y_i\}_{i=1}^{L_1}$:

$$\begin{aligned}&\max\{x_1, x_2, \ldots, x_{L_0}\} - \max\{y_1, y_2, \ldots, y_{L_1}\} - \log_e(L_1)\\ &\quad\le \log_e\left(\sum_{l_0=1}^{L_0} e^{x_{l_0}}\right) - \log_e\left(\sum_{l_1=1}^{L_1} e^{y_{l_1}}\right)\\ &\quad\le \max\{x_1, x_2, \ldots, x_{L_0}\} - \max\{y_1, y_2, \ldots, y_{L_1}\}\\ &\qquad + \log_e(L_0) \quad (17)\end{aligned}$$

If $L_0 \gg L_1$ then, after multiplying (17) by $\frac{1}{L_0}$, the following approximation can be used for sufficiently large L_0:

$$\begin{aligned}&\frac{\log_e\left(\sum_{l_0=1}^{L_0} e^{x_{l_0}}\right) - \log_e\left(\sum_{l_1=1}^{L_1} e^{y_{l_1}}\right)}{L_0}\\ &\quad\approx \frac{\max\{x_1, x_2, \ldots, x_{L_0}\} - \max\{y_1, y_2, \ldots, y_{L_1}\}}{L_0} \quad (18)\end{aligned}$$

Applying (18) to (15) and letting $L_0 = (N_{\mathsf{s}})^{L_{\mathsf{tot}}}$ and $L_1 = (N_{\mathsf{s}})^{ML_{\mathsf{ch}}}$, it follows that the assumption $L_0 \gg L_1$ is satisfied in practical scenarios, and after some manipulations (see [29, Appendix C] for details) we arrive at the approximate LRT (ALRT) detector:

$$\begin{aligned}&\frac{1}{(N_{\mathsf{s}})^{L_{\mathsf{tot}}}}\cdot\Bigg(\min\left\{\mathrm{Tr}\left\{\left(\left(\mathbb{B}[n]\right)^H\cdot\mathbb{C}_{\mathbf{z}}^{-1}\cdot\mathbb{B}[n]\right)\cdot\mathbb{D}_{l_1}^{(\mathsf{sw})}\right\}\right.\\ &\qquad\left.-2\,\mathrm{Re}\left(\sum_{m=0}^{M-1}\left(\tilde{\mathbf{r}}_{N,0}[n\cdot M-m]\right)^H\right.\right.\\ &\qquad\left.\left.\cdot\mathbb{C}_{\mathbf{z}}^{-1}\cdot\mathbb{B}[n]\cdot\tilde{\mathbf{a}}_{\tilde{q}_{(l_1,m)}}\right)\right\}_{l_1=0}^{(N_{\mathsf{s}})^{ML_{\mathsf{ch}}}-1}\\ &\quad-\min\left\{\mathrm{Tr}\left\{\left(\left(\mathbb{B}[n]\right)^H\cdot\mathbb{C}_{\mathbf{z}}^{-1}\cdot\mathbb{B}[n]\right)\cdot\mathbb{D}_{l_0}^{(\mathsf{data})}\right\}\right.\\ &\qquad\left.-2\,\mathrm{Re}\left(\sum_{m=0}^{M-1}\left(\tilde{\mathbf{r}}_{N,0}[n\cdot M-m]\right)^H\right.\right.\\ &\qquad\left.\left.\cdot\mathbb{C}_{\mathbf{z}}^{-1}\cdot\mathbb{B}[n]\cdot\mathbf{a}_{q_{(l_0,m)}}\right)\right\}_{l_0=0}^{(N_{\mathsf{s}})^{L_{\mathsf{tot}}}-1}\Bigg)\\ &\underset{H_1}{\overset{H_0}{\gtrless}}\left(\log_e\left(\lambda\cdot(N_{\mathsf{s}})^{MK}\right)\right)\cdot\frac{1}{(N_{\mathsf{s}})^{L_{\mathsf{tot}}}}\,, \quad (19)\end{aligned}$$

where

$$\begin{aligned}\mathbb{D}_{l_0}^{(\mathsf{data})} &\triangleq \sum_{m=0}^{M-1}\mathbf{a}_{q_{(l_0,m)}}\left(\mathbf{a}_{q_{(l_0,m)}}\right)^H,\\ &\qquad l_0 = 0, 1, \ldots, (N_{\mathsf{s}})^{L_{\mathsf{tot}}} - 1\,, \quad (20a)\\ \mathbb{D}_{l_1}^{(\mathsf{sw})} &\triangleq \sum_{m=0}^{M-1}\tilde{\mathbf{a}}_{\tilde{q}_{(l_1,m)},m}\left(\tilde{\mathbf{a}}_{\tilde{q}_{(l_1,m)},m}\right)^H,\\ &\qquad l_1 = 0, 1, \ldots, (N_{\mathsf{s}})^{ML_{\mathsf{ch}}} - 1\,. \quad (20b)\end{aligned}$$

We note that for a known channel matrix $\mathbb{B}[n]$, the expressions $\mathrm{Tr}\left\{\left(\left(\mathbb{B}[n]\right)^H\cdot\mathbb{C}_{\mathbf{z}}^{-1}\cdot\mathbb{B}[n]\right)\cdot\mathbb{D}_{l_1}^{(\mathsf{sw})}\right\}_{l_1=0}^{(N_{\mathsf{s}})^{ML_{\mathsf{ch}}}-1}$ and $\mathrm{Tr}\left\{\left(\left(\mathbb{B}[n]\right)^H\cdot\mathbb{C}_{\mathbf{z}}^{-1}\cdot\mathbb{B}[n]\right)\cdot\mathbb{D}_{l_0}^{(\mathsf{data})}\right\}_{l_0=0}^{(N_{\mathsf{s}})^{L_{\mathsf{tot}}}-1}$ can be a-priori calculated before frame synchronization begins, which considerably reduces the computational complexity of the ALRT.

B. THE RALRT: REDUCING THE COMPLEXITY OF THE GRID SEARCHES

In order to further reduce the complexity of computing the minimizations, we propose that prior to the application of the post-processing $\mathsf{P}\{\mathbf{r}_{L_{\mathsf{tot}},0}[n]\}$ at the detector input, a simple hard decision detector be applied to $\mathbf{r}_{L_{\mathsf{tot}},0}[n]$, to obtain the estimates:

$$\begin{aligned}\hat{\mathbf{s}}_{L_{\mathsf{tot}},0}^{(\mathsf{data})}[n] &= \underset{\substack{\mathbf{b}_{l_0}^{(\mathsf{data})}\\ l_0=0,1,\ldots,(N_{\mathsf{s}})^{L_{\mathsf{tot}}}-1}}{\mathrm{argmin}}\left\{\|\mathbf{r}_{L_{\mathsf{tot}},0}[n]-\mathbf{b}_{l_0}^{(\mathsf{data})}\|^2\right\}\\ &= \begin{pmatrix}\hat{\mathbf{g}}_{L_{\mathsf{tot}},0}^{(0)}[n]\\ \hat{\mathbf{g}}_{L_{\mathsf{tot}},0}^{(1)}[n]\\ \vdots\\ \hat{\mathbf{g}}_{L_{\mathsf{tot}},0}^{(M-1)}[n]\end{pmatrix}, \quad (21)\end{aligned}$$

where

$$\begin{aligned}\mathbf{b}_{l_0}^{(\mathsf{data})} &\triangleq \begin{pmatrix}\mathbf{a}_{q_{(l_0,0)}}\\ \mathbf{a}_{q_{(l_0,1)}}\\ \vdots\\ \mathbf{a}_{q_{(l_0,M-1)}}\end{pmatrix}\in\mathcal{C}^{L_{\mathsf{tot}}\times 1},\\ &\qquad l_0 = 0, 1, \ldots, (N_{\mathsf{s}})^{L_{\mathsf{tot}}} - 1,\end{aligned}$$

and the estimates

$$\begin{aligned}\hat{\mathbf{s}}_{L_{\mathsf{tot}},0}^{(\mathsf{sw})}[n] &= \underset{\substack{\mathbf{b}_{l_1}^{(\mathsf{sw})}\\ l_1=0,1,\ldots,(N_{\mathsf{s}})^{ML_{\mathsf{ch}}}-1}}{\mathrm{argmin}}\left\{\|\mathbf{r}_{L_{\mathsf{tot}},0}[n]-\mathbf{b}_{l_1}^{(\mathsf{sw})}\|^2\right\}\\ &= \begin{pmatrix}\hat{\hat{\mathbf{g}}}_{L_{\mathsf{tot}},0}^{(0)}[n]\\ \hat{\hat{\mathbf{g}}}_{L_{\mathsf{tot}},0}^{(1)}[n]\\ \vdots\\ \hat{\hat{\mathbf{g}}}_{L_{\mathsf{tot}},0}^{(M-1)}[n]\end{pmatrix}, \quad (22)\end{aligned}$$

where

$$\mathbf{b}_{l_1}^{(\mathsf{sw})} \triangleq \begin{pmatrix} \tilde{\mathbf{a}}_{\tilde{q}(l_1,0),0} \\ \tilde{\mathbf{a}}_{\tilde{q}(l_1,1),1} \\ \vdots \\ \tilde{\mathbf{a}}_{\tilde{q}(l_1,M-1),M-1} \end{pmatrix} \in \mathcal{C}^{L_{\mathsf{tot}} \times 1},$$
$$l_1 = 0, 1, \ldots, (N_{\mathsf{s}})^{ML_{\mathsf{ch}}} - 1,$$

and we note that, by definition of $\mathbf{b}_{l_0}^{(\mathsf{data})}$ and $\mathbf{b}_{l_1}^{(\mathsf{sw})}$, all the elements corresponding to the data belong to $\mathcal{S}$, the constellation set for the transmitted symbols. The vectors $\{\mathbf{b}_{l_0}^{(\mathsf{data})}\}_{l_0=0}^{(N_{\mathsf{s}})^{L_{\mathsf{tot}}}-1}$ represent all the possible combinations of L_{tot} data symbols in an L_{tot}-length vector, and the vectors $\{\mathbf{b}_{l_1}^{(\mathsf{sw})}\}_{l_1=0}^{(N_{\mathsf{s}})^{ML_{\mathsf{ch}}}-1}$ represent all the possible combinations of ML_{ch} data symbols and the transmitted SW of length L_{sw} in an L_{tot}-length vector combined according to the transmission structure. Let $\hat{\mathbf{s}}_{L_{\mathsf{tot}},0}[n]$ represent the hard-decision at the receiver, where it is understood that subject to H_0, $\hat{\mathbf{s}}_{L_{\mathsf{tot}},0}[n] = \hat{\mathbf{s}}_{L_{\mathsf{tot}},0}^{(\mathsf{data})}[n]$, consists only of data symbols and subject to H_1, $\hat{\mathbf{s}}_{L_{\mathsf{tot}},0}[n] = \hat{\mathbf{s}}_{L_{\mathsf{tot}},0}^{(\mathsf{sw})}[n]$, consists of a combination of data symbols and SW symbols taken from $\mathbf{f}_{\mathsf{sw}}$, with the appropriate ordering, while the sub-vectors $\hat{\mathbf{g}}_{L_{\mathsf{tot}},0}^{(m)}[n]$ and $\hat{\tilde{\mathbf{g}}}_{L_{\mathsf{tot}},0}^{(m)}[n]$, $m = 0, 1, \ldots, M-1$, represent hard-decision of the sub-vectors $\mathbf{g}_{L_{\mathsf{tot}},0}^{(m)}[n]$ and $\tilde{\mathbf{g}}_{L_{\mathsf{tot}},0}^{(m)}[n]$, $m = 0, 1, \ldots, M-1$, defined in Eqs. (5) and (13), respectively. Next, we define e_{r_0}, e_{r_1}, $0 \le e_{\mathsf{r}_0} \le N$, $0 \le e_{\mathsf{r}_1} \le L_{\mathsf{ch}}$, $e_{\mathsf{r}_0}, e_{\mathsf{r}_1} \in \mathcal{N}$, with which we construct the sets $\mathcal{Q}_0$, $\mathcal{Q}_1$, to contain all the vectors $\mathbf{b}_{l_0}^{(\mathsf{data})}$ and $\mathbf{b}_{l_1}^{(\mathsf{sw})}$, respectively, that are composed of the sub-vectors $\mathbf{a}_{q(l_0,m)}$ and $\tilde{\mathbf{a}}_{\tilde{q}(l_1,0),m}$, $m = 0, 1, \ldots, M-1$, respectively, with a maximum of e_{r_0} or e_{r_1} different coordinates from the hard-decision sub-vectors $\hat{\mathbf{g}}_{L_{\mathsf{tot}},0}^{(m)}[n]$ and $\hat{\tilde{\mathbf{g}}}_{L_{\mathsf{tot}},0}^{(m)}[n]$, $m = 0, 1, \ldots, M-1$, respectively. In order to write mathematically the construction of the sets $\mathcal{Q}_0$, $\mathcal{Q}_1$, we define the indicator function $I(b)$, $I(b) = 1$ if $b = 0$ and $I(b) = 0$ if $b \neq 0$, $b \in \mathcal{C}$, and for a vector $\mathbf{v} = (v_1, v_2, \ldots, v_n)^T$, $\mathbf{v} \in \mathcal{C}^{n \times 1}$, let $I(\mathbf{v}) = \big(I(v_1), I(v_2), \ldots, I(v_n)\big)^T$. Accordingly, the sets $\mathcal{Q}_0$, $\mathcal{Q}_1$ are mathematically defined as:

$$\mathbf{b}_{l_0}^{(\mathsf{data})} \in \mathcal{Q}_0, \ \text{if} \ \Big(I\big(\hat{\mathbf{g}}_{L_{\mathsf{tot}},0}^{(m)}[n] - \mathbf{a}_{q(l_0,m)}\big)\Big)^T \cdot I\big(\hat{\mathbf{g}}_{L_{\mathsf{tot}},0}^{(m)}[n] - \mathbf{a}_{q(l_0,m)}\big) \le e_{\mathsf{r}_0},$$
$$\forall m = 0, 1, \ldots M-1, \ l_0 = 0, 1, \ldots, (N_{\mathsf{s}})^{L_{\mathsf{tot}}} - 1. \quad (23)$$

$$\mathbf{b}_{l_1}^{(\mathsf{sw})} \in \mathcal{Q}_1, \ \text{if} \ \Big(I\big(\hat{\tilde{\mathbf{g}}}_{L_{\mathsf{tot}},0}^{(m)}[n] - \tilde{\mathbf{a}}_{\tilde{q}(l_1,0),m}\big)\Big)^T \cdot I\big(\hat{\tilde{\mathbf{g}}}_{L_{\mathsf{tot}},0}^{(m)}[n] - \tilde{\mathbf{a}}_{\tilde{q}(l_1,0),m}\big) \le e_{\mathsf{r}_1},$$
$$\forall m = 0, 1, \ldots M-1, \ l_1 = 0, 1, \ldots, (N_{\mathsf{s}})^{ML_{\mathsf{ch}}} - 1. \quad (24)$$

The two minimizations in (19) are now evaluated using only the sequences in the sets $\mathcal{Q}_0$, $\mathcal{Q}_1$, whose sizes are determined by the parameters e_{r_0} and e_{r_1}. Therefore, by decreasing e_{r_0}, e_{r_1}, we can decrease the number of sequences used in the computation of the ALRT, which reduces the computational complexity at the cost of a decrease in optimally of the ALRT detector stated in (19). The sets of indexes $\mathcal{L}_0$, $\mathcal{L}_1$ for the new grid search follow from the sets $\mathcal{Q}_0$, $\mathcal{Q}_1$, respectively, as:

$$l_0 \in \mathcal{L}_0 \ \text{iff} \ \mathbf{b}_{l_0}^{(\mathsf{data})} \in \mathcal{Q}_0, \ \ l_0 = 0, 1, \ldots, (N_{\mathsf{s}})^{L_{\mathsf{tot}}} - 1 \quad (25)$$
$$l_1 \in \mathcal{L}_1 \ \text{iff} \ \mathbf{b}_{l_1}^{(\mathsf{sw})} \in \mathcal{Q}_1, \ \ l_1 = 0, 1, \ldots, (N_{\mathsf{s}})^{ML_{\mathsf{ch}}} - 1. \quad (26)$$

Evaluating the ALRT detector within the reduced grid search will be referred to in the following as the reduced approximate LRT (RALRT), which is stated as:

$$\frac{1}{(N_{\mathsf{s}})^{L_{\mathsf{tot}}}} \cdot \Bigg(\min \Bigg\{ \mathrm{Tr}\Bigg\{ \Big(\big(\mathbb{B}[n]\big)^H \cdot \mathbb{C}_{\mathbf{z}}^{-1} \cdot \mathbb{B}[n] \Big) \cdot \mathbb{D}_{l_1}^{(\mathsf{sw})} \Bigg\} - 2\,\mathrm{Re}\Bigg(\sum_{m=0}^{M-1} \big(\tilde{\mathbf{r}}_{N,0}[n \cdot M - m]\big)^H \cdot \mathbb{C}_{\mathbf{z}}^{-1} \cdot \mathbb{B}[n] \cdot \tilde{\mathbf{a}}_{\tilde{q}(l_1,m)} \Bigg) \Bigg\}_{l_1 \in \mathcal{L}_1}$$
$$- \min \Bigg\{ \mathrm{Tr}\Bigg\{ \Big(\big(\mathbb{B}[n]\big)^H \cdot \mathbb{C}_{\mathbf{z}}^{-1} \cdot \mathbb{B}[n] \Big) \cdot \mathbb{D}_{l_0}^{(\mathsf{data})} \Bigg\} - 2\,\mathrm{Re}\Bigg(\sum_{m=0}^{M-1} \big(\tilde{\mathbf{r}}_{N,0}[n \cdot M - m]\big)^H \cdot \mathbb{C}_{\mathbf{z}}^{-1} \cdot \mathbb{B}[n] \cdot \mathbf{a}_{q(l_0,m)} \Bigg) \Bigg\}_{l_0 \in \mathcal{L}_0} \Bigg)$$
$$\underset{H_1}{\overset{H_0}{\gtrless}} \Big(\log_e \big(\lambda \cdot (N_{\mathsf{s}})^{MK} \big) \Big) \cdot \frac{1}{(N_{\mathsf{s}})^{L_{\mathsf{tot}}}} \,. \quad (27)$$

C. COMPUTATIONAL COMPLEXITY OF THE ALRT AND THE RALRT

The computational complexities of the ALRT and the RALRT were also derived in [29, Appendix D] for the purpose of comparing the computational complexity of the different detectors. It is concluded that the total complexity of the ALRT detector in Eq. (19) is:

$$\mathrm{CM}\big(\mathrm{ALRT}\big) = \big(MK \cdot (N+1) + 1\big) \cdot \big((N_{\mathsf{s}})^{L_{\mathsf{tot}}} + (N_{\mathsf{s}})^{ML_{\mathsf{ch}}}\big) + 1$$
$$\mathrm{CA}\big(\mathrm{ALRT}\big) = M \cdot \big((N-1) \cdot K + (K-1)\big) \cdot \big((N_{\mathsf{s}})^{L_{\mathsf{tot}}} + (N_{\mathsf{s}})^{ML_{\mathsf{ch}}}\big) + 1.$$

For the RALRT detector in Eq. (27) the computational complexity is equal to:

$$\mathrm{CM}\big(\mathrm{RALRT}\big) = \big(MK \cdot (N+1) + 1\big) \cdot \big(|\mathcal{Q}_1| + |\mathcal{Q}_0|\big) + 1$$
$$\mathrm{CA}\big(\mathrm{RALRT}\big) = M \cdot \big((N-1) \cdot K + (K-1)\big) \cdot \big(|\mathcal{Q}_1| + |\mathcal{Q}_0|\big) + 1.$$

In Section VII we show via numerical simulations that the proposed complexity reduction approach of the RALRT can provide at least an order of magnitude reduction in complexity w.r.t. the ALRT without a noticeable loss in detection performance.

VI. NOVEL SALRT FRAME SYNCHRONIZATION ALGORITHM: LOWERING COMPLEXITY WITHOUT CHANNEL KNOWLEDGE

The major disadvantage of the RALRT (27) as well as of the LRT (15) is that they require knowledge of the CIR. However, as frame synchronization is typically the initial step in reception, it is not likely that the receiver has a reliable estimate of the CIR at the time in which it attempts to synchronize with the beginning of the frame. We note that we assume that the statistical properties of the noise vary much slower than the channel, hence they *do not change throughout the time duration it takes to synchronize*. Consequently, the receiver is assumed to have a reliable estimate of the noise correlation function prior to synchronization. In the following we derive a suboptimal detector based on (15) with a significantly reduced computational complexity, which can be applied also to scenarios in which the matrix $\mathbb{B}[n]$, which contains the CIR information needed for computing the LRT, is unknown. To overcome this difficulty, we propose a channel estimation procedure which facilitates implementation of the LRT without an apriori knowledge of the CIR.

A. BLIND ESTIMATION OF THE CHANNEL MATRIX

In this section we address the lack of knowledge of the channel matrix $\mathbb{B}[n]$ which is needed for computing the RALRT in (27). To overcome this issue, we propose to estimate the CIR coefficients. We note that as most of the signal parameters are not synchronized at this point, such an estimation will typically be very noisy, and therefore it is not expected to facilitate sufficient decoding performance. Nevertheless, the simulation study reported in Section VII demonstrates that this noisy estimation is completely sufficient for obtaining good FS performance. In order to estimate the CIR for computing the LRT, we process L_{EQ} received samples as depicted in Fig. 4, where $L_{\mathsf{tot}} < L_{\mathsf{EQ}} < L_{\mathsf{d}} - ML_{\mathsf{ch}}$, to obtain an estimate of $L_{\mathsf{est}} = L_{\mathsf{EQ}} - P_{\mathsf{h}} \cdot L_{\mathsf{ch}}$ information symbols via the blind equalization scheme proposed in [34, Eq. (28)], [35, Ch. 10.5-2]. To that aim, the receiver first collects L_{tot} samples of the received signal $r[m]$, required for generating $\mathbf{r}_{L_{\mathsf{tot}},0}[n]$, as depicted in Fig. 4. Before computing the LRT, additional $L_{\mathsf{EQ}} = J \cdot P_{\mathsf{h}}$, $J = \xi \cdot (L_{\mathsf{ch}}+1)$, $\xi \geq 3$, $\xi \in \mathcal{N}$ samples are collected to facilitate the application of the equalizer proposed in [34, Eq. (28)], [35, Ch. 10.5-2]. Define next the following vectors:

$$\mathbf{r}_{\mathsf{eqz}}^{(i,l)}[n] \triangleq \begin{pmatrix} r[n-i] \\ r[n-P_{\mathsf{h}}-i] \\ r[n-2\cdot P_{\mathsf{h}}-i] \\ \vdots \\ r[n-l\cdot P_{\mathsf{h}}-i] \end{pmatrix} \in \mathcal{C}^{(l+1)\times 1},$$
$$i = 0,1,\ldots,P_{\mathsf{h}}-1,\ l \in \mathcal{N}$$
$$\mathbf{u}^{(i,k)} \triangleq \begin{pmatrix} u_0^{(i,k)} \\ u_1^{(i,k)} \\ \vdots \\ u_{L_{\mathsf{ch}}}^{(i,k)} \end{pmatrix} \in \mathcal{C}^{(L_{\mathsf{ch}}+1)\times 1},$$
$$i = 0,1,\ldots,P_{\mathsf{h}}-1,\ k = 0,1,\ldots,J-(L_{\mathsf{ch}}+1).$$

$\mathbf{u}^{(i,k)}$ represents the equalizer taps at iteration number k for the input $\mathbf{r}_{\mathsf{eqz}}^{(i,L_{\mathsf{ch}})}[n]$, corresponding to the i'th time instant within the period of the channel (which consists of P_{h} time instants). Accordingly, we define the equalizer output after the k'th iteration as:

$$\hat{d}^{(i,k)} = \left(\mathbf{u}^{(i,k)}\right)^T \cdot \mathbf{r}_{\mathsf{eqz}}^{(i,L_{\mathsf{ch}})}[n-k\cdot P_{\mathsf{h}}],$$
$$i = 0,1,\ldots,P_{\mathsf{h}}-1,\ k = 0,1,\ldots,J-(L_{\mathsf{ch}}+2). \quad (28)$$

For each time instant within the channel period P_{h}, the iterative update equation for the equalizer is given by:

$$\mathbf{u}^{(i,k+1)} = \mathbf{u}^{(i,k)} + \Delta_p \cdot \left(\mathbf{r}_{\mathsf{eqz}}^{(i,L_{\mathsf{ch}})}[n-k\cdot P_{\mathsf{h}}]\right)^* \cdot \hat{d}^{(i,k)} \cdot (\gamma_{\mathsf{s}}^2 - |\hat{d}^{(i,k)}|^2),$$
$$i = 0,1,\ldots,P_{\mathsf{h}}-1,\ k = 0,1,\ldots,J-(L_{\mathsf{ch}}+2),$$
$$\gamma_{\mathsf{s}}^2 \triangleq \frac{\mathbb{E}\left[|s[m]|^4\right]}{\mathbb{E}\left[|s[m]|^2\right]}, \quad (29)$$

where $\Delta_p \in \mathcal{R}^{++}$ is the equalizer's step size, which is selected in order to ensure convergence for the relevant scenarios [36], while attaining a sufficiently small mean squared error (MSE). The initial vector of equalizer taps for the iterative algorithm, $\mathbf{u}^{(i,0)}$, is set to $\mathbf{u}^{(i,0)} = \left(u_0^{(i,0)}, u_1^{(i,0)}, \ldots, u_{L_{\mathsf{ch}}}^{(i,0)}\right)^T = (1,0,\ldots,0)^T$, $i = 0,1,\ldots,P_{\mathsf{h}}-1$. The iterative algorithm output is $\mathbf{u}^{(i,J-(L_{\mathsf{ch}}+1))}$, which is then used for estimating the L_{est} information symbols from the received L_{EQ} samples via a hard decision rule:

$$\hat{s}\left[n-k\cdot P_{\mathsf{h}}-i\right] = \underset{\rho\in\mathcal{S}}{\operatorname{argmin}} \left\| \left(\mathbf{u}^{\left(i,J-(L_{\mathsf{ch}}+1)\right)}\right)^T \cdot \mathbf{r}_{\mathsf{eqz}}^{(i,L_{\mathsf{ch}})}[n-k\cdot P_{\mathsf{h}}] - \rho \right\|^2,$$
$$i = 0,1,\ldots,P_{\mathsf{h}}-1,\ k = 0,1,\ldots,J-(L_{\mathsf{ch}}+1). \quad (30)$$

Next we define $\Psi \in \mathcal{N}$ as the smallest integer satisfying $\Psi \cdot P_{\mathsf{h}} > L_{\mathsf{ch}}+1$ and the matrices $\hat{\mathbb{G}}^{(i)}[n] \in \mathcal{C}^{(\Omega+1)\times(L_{\mathsf{ch}}+1)}$, $\Omega = \left(J-(L_{\mathsf{ch}}+\Psi)\right)$, $i = 0,1,\ldots,P_{\mathsf{h}}-1$ as follows:

$$\left[\hat{\mathbb{G}}^{(i)}[n]\right]_{a_1+1,a_2+1} \triangleq \hat{s}\left[n-a_1\cdot P_{\mathsf{h}}-a_2-i\right],$$
$$a_1 = 0,1,\ldots,\Omega,\ a_2 = 0,1,\ldots,L_{\mathsf{ch}}.$$

With these quantities we estimate a single period of the CIR, $\tilde{\mathbf{h}}[n,k]$ defined in (10), via a least sum of squared errors (LSSE) channel estimator [37], [38, Eq. (16)], that is:

$$\hat{\tilde{\mathbf{h}}}[n,i] = \left((\hat{\mathbb{G}}^{(i)}[n])^H \cdot \hat{\mathbb{G}}^{(i)}[n]\right)^{-1} \cdot \left(\hat{\mathbb{G}}^{(i)}[n]\right)^H \cdot \mathbf{r}_{\mathsf{eqz}}^{(i,\Omega)}[n],$$
$$i = 0,1,\ldots,P_{\mathsf{h}}-1. \quad (31)$$

Lastly, using the periodicity of the CIR $\hat{\tilde{\mathbf{h}}}[n,i] = \hat{\tilde{\mathbf{h}}}[n,i+P_{\mathsf{h}}]$, the entire estimated channel matrix $\hat{\mathbb{B}}[n]$ is constructed via Eq. (10). Lastly, applying the estimated CIR to the RALRT

we obtain the suboptimal approximate LRT, denoted as SALRT, which is expressed as:

$$\begin{aligned}
&\frac{1}{(N_{\mathsf{s}})^{L_{\mathsf{tot}}}}\cdot\Bigg(\min\Bigg\{\mathrm{Tr}\Bigg\{\Big(\big(\hat{\mathbb{B}}[n]\big)^{H}\cdot\mathbb{C}_{\mathsf{z}}^{-1}\cdot\hat{\mathbb{B}}[n]\Big)\cdot\mathbb{D}_{l_1}^{(\mathsf{sw})}\Bigg\}\\
&\qquad -2\,\mathrm{Re}\Big(\sum_{m=0}^{M-1}\Big(\tilde{\mathbf{r}}_{N,0}[n\cdot M-m]\Big)^{H}\\
&\qquad\cdot\mathbb{C}_{\mathsf{z}}^{-1}\cdot\hat{\mathbb{B}}[n]\cdot\tilde{\mathbf{a}}_{\tilde{q}_{(l_1,m)},m}\Big)\Bigg\}_{l_1\in\mathcal{L}_1}\\
&-\min\Bigg\{\mathrm{Tr}\Bigg\{\Big(\big(\hat{\mathbb{B}}[n]\big)^{H}\cdot\mathbb{C}_{\mathsf{z}}^{-1}\cdot\hat{\mathbb{B}}[n]\Big)\cdot\mathbb{D}_{l_0}^{(\mathsf{data})}\Bigg\}\\
&\qquad -2\,\mathrm{Re}\Big(\sum_{m=0}^{M-1}\Big(\tilde{\mathbf{r}}_{N,0}[n\cdot M-m]\Big)^{H}\\
&\qquad\cdot\mathbb{C}_{\mathsf{z}}^{-1}\cdot\hat{\mathbb{B}}[n]\cdot\mathbf{a}_{q_{(l_0,m)}}\Big)\Bigg\}_{l_0\in\mathcal{L}_0}\Bigg)\\
&\underset{H_1}{\overset{H_0}{\gtrless}}\Big(\log_e\Big(\lambda\cdot(N_{\mathsf{s}})^{MK}\Big)\Big)\cdot\frac{1}{(N_{\mathsf{s}})^{L_{\mathsf{tot}}}}
\end{aligned}\tag{32}$$

B. SUMMARY: THE STEPS OF THE SALRT FRAME SYNCHRONIZATION ALGORITHM

Initialization: The receiver obtains the following parameters:

- $\mathcal{S}$ - Constellation set of transmitted symbols.
- $[f_0, f_1, .., f_{L_{\mathsf{sw}}-1}]$ - Transmitted SW.
- M - Number the SW sub-blocks.
- P_{h} - The period of the CIR.
- P_{z} - The period of the ACGN correlation function.
- L_{ch} - Length of channel memory.
- N - A common multiple of the discrete periods of the CIR and ACGN correlation function, P_{h} and P_{z}, which satisfies $k_1P_{\mathsf{h}}=k_2P_{\mathsf{z}}=N,\ k_1,k_2\in\mathcal{N},$ with $N>L_{\mathsf{ch}}$. We note that this parameter can be computed independently by the receiver.
- $\mathbb{C}_{\mathsf{z}}\in\mathcal{R}^{K\times K}$ - The covariance matrix of the ACGN, $K=N-L_{\mathsf{ch}}$.
- e_{r_0}, e_{r_1} - Control parameters for the cardinality of the grid search sets, $\mathcal{Q}_0$ and $\mathcal{Q}_1$.

Remark 1: In general, N and L_{ch} are sufficient for applying the algorithm. Knowledge of P_{h} can reduce the complexity of the channel estimation step, as it facilitates the estimation of a single period of the CIR via (31)*, and then obtaining all required N CIR values for constructing the matrix $\mathbb{B}[n]$ by using the periodicity of the CIR. Without such knowledge, the estimator* (31) *has to be applied N times, where $N>P_{\mathsf{h}}$.*

Remark 2: While L_{ch} may be over estimated, the period of the model can be estimated by dedicated blind algorithms e.g, [39]. If the channel is not periodic, then the algorithm is directly applicable without the need for the period estimation part.

Steps of the SALRT Algorithm: The steps of the proposed suboptimal approximate LRT frame synchronization detector are detailed below:

1) Construct the matrices $\mathbb{D}_{l_0}^{(\mathsf{data})}$, $l_0=0,1,\ldots,(N_{\mathsf{s}})^{L_{\mathsf{tot}}}-1$ and $\mathbb{D}_{l_1}^{(\mathsf{sw})}$, $l_1=0,1,\ldots,(N_{\mathsf{s}})^{ML_{\mathsf{ch}}}-1$, via Eqs. (20a) and (20b).
2) Collect L_{tot} channel output samples to assemble $\mathbf{r}_{L_{\mathsf{tot}},0}[n]$, the incoming vector samples.
3) Estimate channel matrix $\mathbb{B}[n]$:
   a) Collect additional L_{EQ} channel output samples as depicted in Fig. 4, and compute the finite impulse response (FIR) of the channel equalizer, $\mathbf{u}^{(i,J-(L_{\mathsf{ch}}+1))}$, via Eqs. (28) and (29).
   b) Using $\mathbf{u}^{(i,J-(L_{\mathsf{ch}}+1))}$ estimate the $L_{\mathsf{est}}=L_{\mathsf{EQ}}-P_{\mathsf{h}}\cdot L_{\mathsf{ch}}$ transmitted symbols from the L_{EQ} channel output samples via Eq. (30).
   c) Estimate the CIR vectors, $\tilde{\mathbf{h}}[n,i]$, $i=0,1,\ldots,P_{\mathsf{h}}-1$ via Eq. (31), and construct the estimated channel matrix, $\hat{\mathbb{B}}[n]$ via Eq. (10).
4) Reducing the complexity of the grid search:
   a) From $\mathbf{r}_{L_{\mathsf{tot}},0}[n]$, evaluate the hard decision estimates $\hat{\mathbf{s}}_{L_{\mathsf{tot}},0}^{(\mathsf{data})}[n]$ and $\hat{\mathbf{s}}_{L_{\mathsf{tot}},0}^{(\mathsf{sw})}[n]$, via Eqs. (21), (22).
   b) Compute the sets of indexes $\mathcal{L}_0$, $\mathcal{L}_1$ for the new grid search via Eqs. (23), (24), (25) and (26).
5) Apply post-processing to $\mathbf{r}_{L_{\mathsf{tot}},0}[n]$ according to Eq. (9), and obtain $\mathsf{P}\{\mathbf{r}_{L_{\mathsf{tot}},0}[n]\}=\mathbf{r}_{L_{\mathsf{tot}},0}^{(\mathsf{P})}[n]$.
6) Evaluate the SALRT and choose between H_0 and H_1 via Eq. (32).

C. COMPLEXITY OF THE SALRT DETECTOR AND COMPARISONS WITH OTHER DETECTORS

The computational complexity of the proposed SALRT detector is detailed in terms of the CMs and of the CAs for each step of the algorithm, in [29, Table III], where the details of the derivations are provided in [29, Appendix D]. It follows from [29, Appendix D] that the total complexity of the SALRT detector in Eq. (32) is equal to:

$$\begin{aligned}
&\mathrm{CM}\big(\mathrm{SALRT}\big)\\
&=\big(MK\cdot(N+1)+1+N^3\big)\cdot\big(|\mathcal{Q}_1|+|\mathcal{Q}_0|\big)\\
&\quad+KN\cdot(K+N)+1\\
&\quad+P_{\mathsf{h}}\cdot\big(J-(L_{\mathsf{ch}}+1)\big)\cdot\big(2\cdot(L_{\mathsf{ch}}+1)+3\big)\\
&\quad+P_{\mathsf{h}}\cdot\big(L_{\mathsf{ch}}+2\big)\cdot\big((\Omega+1)\cdot(L_{\mathsf{ch}}+1)+(L_{\mathsf{ch}}+1)^2\big)\\
&\quad+(L_{\mathsf{EQ}}-P_{\mathsf{h}}\cdot L_{\mathsf{ch}})\cdot(N_{\mathsf{s}}+L_{\mathsf{ch}}+1)+\big(c_1+c_2\big)\cdot L_{\mathsf{tot}}\\
&\mathrm{CA}\big(\mathrm{SALRT}\big)\\
&=\big(M\cdot\big((N-1)\cdot K+(K-1)\big)+(N-1)\cdot N^2+N\big)\\
&\qquad\cdot\big(|\mathcal{Q}_1|+|\mathcal{Q}_0|\big)\\
&\quad+N\cdot(K-1)\cdot(K+N)+1\\
&\quad+P_{\mathsf{h}}\cdot\big(J-(L_{\mathsf{ch}}+1)\big)\cdot\big(2\cdot(L_{\mathsf{ch}}+1)\big)\\
&\quad+P_{\mathsf{h}}\cdot\big(\Omega\cdot(L_{\mathsf{ch}}+1)\cdot(L_{\mathsf{ch}}+2)\\
&\qquad+L_{\mathsf{ch}}\cdot(L_{\mathsf{ch}}+1)+(L_{\mathsf{ch}})^3\big)\\
&\quad+(L_{\mathsf{EQ}}-P_{\mathsf{h}}\cdot L_{\mathsf{ch}})\cdot(N_{\mathsf{s}}+L_{\mathsf{ch}})\\
&\quad+\big(c_1+c_2\big)\cdot(2L_{\mathsf{tot}}-1)
\end{aligned}$$

As explained in [29, Appendix D], $c_1 \ll (N_{\mathsf{s}})^{L_{\mathsf{tot}}}$ and $c_2 \ll (N_{\mathsf{s}})^{ML_{\mathsf{ch}}}$, $c_1, c_2 \in \mathcal{N}$, are constants that can be computed from the constellation set $\mathcal{S}$ used for transmission.

A very common detector for frame synchronization in channels with memory is based on the correlation metric [23]:

$$\mathrm{Corr}\left(\mathbf{r}^{(\mathsf{cor})}_{L_{\mathsf{sw}},0}[n]\right) = \left\| \left(\mathbf{r}^{(\mathsf{cor})}_{L_{\mathsf{sw}},0}[n]\right)^{H} \cdot \mathbf{f}_{\mathsf{sw}} \right\|^2 \underset{H_1}{\overset{H_0}{\gtrless}} \lambda \,, \quad (33)$$

where $\mathbf{r}^{(\mathsf{cor})}_{L_{\mathsf{sw}},0}[n] \in \mathcal{C}^{L_{\mathsf{sw}} \times 1}$ is a vector of the received channel outputs, where transmission is applied without the pre-processing and the post-processing procedures described in Section III. The total complexity of the correlator detector of Eq. (33) is shown in [29, Appendix D] to be:

$$\begin{aligned} \mathrm{CM}\big(\mathrm{Corr}\big) &= L_{\mathsf{sw}} + 1 \\ \mathrm{CA}\big(\mathrm{Corr}\big) &= L_{\mathsf{sw}} - 1 \,. \end{aligned}$$

We compare the computational complexity expressions of the different schemes considered focusing on the number of CMs, as a CM takes more systems resources to implement than a CA [40]. Comparing and $\mathrm{CM}\big(\mathrm{SALRT}\big)$ with $\mathrm{CM}\big(\mathrm{LRT}\big)$ (see Section IV-C), $\mathrm{CM}\big(\mathrm{ALRT}\big)$, $\mathrm{CM}\big(\mathrm{RALRT}\big)$ (see Section V-C), and with $\mathrm{CM}\big(\mathrm{Corr}\big)$, we observe that the computational complexity of ALRT detector is a somewhat smaller than the computational complexity of the LRT detector, but the computational complexity of the RALRT detector is much smaller than that of LRT and of the ALRT detectors since $\big(|\mathcal{Q}_1| + |\mathcal{Q}_0|\big) \ll \big((N_{\mathsf{s}})^{L_{\mathsf{tot}}} + (N_{\mathsf{s}})^{ML_{\mathsf{ch}}}\big)$. The computational complexity of the SALRT detector is higher than that of the RALRT detector since SALRT estimates the CIR prior to applying the RALRT detector. Nevertheless, this complexity is much smaller than that of the ALRT, and of the LRT detectors, since it does not depend on the quantity $\big((N_{\mathsf{s}})^{L_{\mathsf{tot}}} + (N_{\mathsf{s}})^{ML_{\mathsf{ch}}}\big)$, which is the dominant term in the computational complexity of the ALRT and LRT detectors. Lastly, we note that the correlator detector has the lowest computational complexity among all the detectors considered above.

Table 1 summarizes the complexity order for the different detectors as a function of the length of the SW, L_{sw}, and the number of blocks into which the SW is partitioned, M. We note that while for each detector, the exact number of CMs differs from the exact number of CAs, their asymptotics w.r.t. L_{sw} and M is the same. Accordingly, we refer to this asymptotics in Table 1 as "CM/CA complexity order". Examining Table 1, we first observe that CM/CA complexity orders for the LRT and for the ALRT are exponentially dependent on M and on L_{sw}. This is because these parameters determine the search space for these algorithms. The CM/CA complexity orders of the RALRT and of the SALRT are inversely proportional to M, which follows as when M increases the dimensions of the operations used in these estimators decrease. The CM/CA complexity orders for the RALRT, the SALRT and the correlator are polynomial in L_{sw}, where for the correlator the CM/CA complexity orders increase linearly in L_{sw}, for the RALRT the CM/CA complexity orders increase as the square of L_{sw} and for the SALRT the CM/CA complexity orders increase as the cubic power of L_{sw}. Thus, the approximation used for the RALRT decreases the CM/CA complexity orders from exponential to polynomial, yet it is an order of magnitude larger than that of the correlator – which evidently has very low CM/CA complexity orders. The CM/CA complexity of the SALRT is an order of magnitude larger than that of the RALRT, which is due to the additional complexity required for channel estimation.

TABLE 1. Computational complexity order for the different detectors.

Detector	CM/CA complexity order
LRT	$\mathcal{O}\left(\frac{2}{M} \cdot (N_{\mathsf{s}})^{ML_{\mathsf{ch}}} \cdot \left(L^2_{\mathsf{sw}} \cdot (N_{\mathsf{s}})^{L_{\mathsf{sw}}}\right)\right)$
ALRT	$\mathcal{O}\left(\frac{1}{M} \cdot (N_{\mathsf{s}})^{ML_{\mathsf{ch}}} \cdot \left(L^2_{\mathsf{sw}} \cdot (N_{\mathsf{s}})^{L_{\mathsf{sw}}}\right)\right)$
RALRT	$\mathcal{O}\left(\frac{1}{M} \cdot \lvert\mathcal{Q}_0\rvert \cdot L^2_{\mathsf{sw}}\right)$
Correlator	$\mathcal{O}\left(L_{\mathsf{sw}}\right)$
SALRT	$\mathcal{O}\left(\frac{1}{M} \cdot \lvert\mathcal{Q}_0\rvert \cdot (L^2_{\mathsf{sw}} + L^3_{\mathsf{sw}})\right)$

VII. NUMERICAL EXAMPLES AND DISCUSSION

In this section we compare the performance of the three proposed algorithms for frame synchronization, the ALRT stated in Eq. (19), the RALRT stated in Eq. (27) and the SALRT stated in Eq. (32), together with the performance of the optimal LRT detector derived in Eq. (15), and with the widely adopted correlation metric detector [23], stated in Eq. (33). The performance of hypothesis testing detectors are evaluated via their receiver operating characteristics (ROC) [31] and the area under the curve (AUC) of the ROC, where a larger AUC is associated with a better detector [41]. The ROC plots depict the probability of successfully detecting a SW when it is present (i.e., given that the H_1 hypothesis is true), denoted with p_{d}, vs. the probability of declaring SW detection when no SW is present (i.e., when the H_0 hypothesis is true), denoted with p_{fa}. We tested the performance of the algorithms for two different scenarios: The first scenario, referred to hereafter as 'Scenario 1', consists of a non-periodic CIR and WSS additive noise, and the second scenario, referred to hereafter as 'Scenario 2', consists of a periodic CIR and ACGN, as described in Section III. The transmitted symbols are selected from a BPSK constellation, $\mathcal{S} = \{-1, 1\}$, and accordingly $N_{\mathsf{s}} = 2$. The parameters of the simulated channels are as follows:

Scenario 1:

We consider a slowly time-varying frequency-selective fading channel, such that the CIR remains constant throughout the transmission of each frame. The CIR, $h[m, l]$, has complex values taken from [42, Table 1]:

$$\begin{aligned} &h[m,0] = 1.05 - 0.82j,\ h[m,1] = 0.71 + 0.45j, \\ &h[m,2] = 0.63 - 0.72j, \quad \forall m \in \mathcal{Z}, \\ &h[m,k] = 0,\ k \neq \{0,1,2\}, \quad \forall\, m \in \mathcal{Z}. \end{aligned}$$

Accordingly, the channel period is $P_{\mathsf{h}} = 1$ with a finite memory $L_{\mathsf{h}} = 2$. The noise is a zero-mean baseband proper complex, additive WSS Gaussian process, with a finite memory $L_{\mathsf{z}} = 2$, and with the following correlation function:

$$\begin{aligned} c_{\mathsf{z}}[m,l] &= \sigma_z^2 \cdot \delta[l] + 0.5 \cdot \sigma_z^2 \cdot \delta[l+1] \\ &\quad + 0.5 \cdot \sigma_z^2 \cdot \delta[l-1] + 0.3 \cdot \sigma_z^2 \cdot \delta[l+2] \\ &\quad + 0.3 \cdot \sigma_z^2 \cdot \delta[l-2],\ \sigma_z \in \mathcal{R}^{++},\ m, l \in \mathcal{Z}, \end{aligned}$$

where σ_z^2 is selected to satisfy the target signal-to-noise ratio (SNR), which is given by

$$SNR = \frac{\sigma_s^2}{\sigma_z^2 \cdot L_{\mathsf{tot}}} \cdot \mathrm{Tr}\left\{ \left(\mathbb{A}_{L_{\mathsf{tot}},0}[n]\right)^H \cdot \mathbb{A}_{L_{\mathsf{tot}},0}[n] \right\}. \quad (34)$$

Since the corresponding noise correlation matrix does not depend on m, its period is $P_{\mathsf{z}} = 1$. The memory of the channel is $L_{\mathsf{ch}} = \max\{L_{\mathsf{z}}, L_{\mathsf{h}}\} = 2$ and the period of the channel, denoted with N, is the LCM of the discrete periods P_{h} and P_{z} that satisfies $N > L_{\mathsf{ch}}$, that is $N \geq 3$. We choose $N = 8$ to facilitate a reasonable partition (not too fragmented) of the SW as will be described later in this section. The noise correlation matrix, $\mathbb{C}_{\mathsf{z}}$ is defined in Eq. (38), where $K = N - L_{\mathsf{ch}} = 8 - 2 = 6$.

Scenario 2:

We consider a time-varying frequency selective fading channel, such that the channel is LPTV with a complex CIR, $h[m,l]$, whose values are taken from [42, Table 1]:

$$\begin{aligned} h[2\cdot m_1, 0] &= 1.05 - 0.82j, \\ h[2\cdot m_1, 1] &= 0.71 + 0.45j, \\ h[2\cdot m_1, 2] &= 0.63 - 0.72j, \\ h[2\cdot m_1 + 1, 0] &= 0.53 + 0.62j, \\ h[2\cdot m_1 + 1, 1] &= 0.41 + 0.37j, \\ h[2\cdot m_1 + 1, 2] &= 0.20 - 0.34j, \quad \forall m_1 \in \mathcal{Z}, \\ h[m_2, k_2] &= 0,\ k_2 \neq \{0,1,2\}, \quad \forall\, m_2 \in \mathcal{Z}. \end{aligned}$$

Accordingly the channel period is $P_{\mathsf{h}} = 2$ with a finite memory $L_{\mathsf{h}} = 2$. The noise is a zero mean, baseband proper complex ACGN process with a period $P_{\mathsf{z}} = 8$, and a finite correlation memory of $L_{\mathsf{z}} = 2$, and is generated by filtering a memoryless proper complex WSCS Gaussian process with zero mean and variance:

$$\sigma_z^2[m] = \tilde{\sigma}_z^2 \cdot \left(2 + \cos\left(\frac{2\pi}{P_{\mathsf{z}}} \cdot m\right)\right),\ \tilde{\sigma}_z \in \mathcal{R}^{++}, \quad \forall m \in \mathcal{Z},$$

where $\tilde{\sigma}_z^2$ is selected according to the target SNR. The filter used for noise generation is a casual LTI filter, denoted $h_{\mathsf{z}}[m]$, with an exponentially decaying CIR:

$$\begin{aligned} &h_{\mathsf{z}}[0] = 0.6,\ h_{\mathsf{z}}[1] = 0.2, \quad h_{\mathsf{z}}[2] = 0.066, \\ &h_{\mathsf{z}}[k] = 0 \text{ for } k \neq \{0,1,2\}, \quad k \in \mathcal{Z}, \end{aligned}$$

resulting in $L_{\mathsf{z}} = 2$. The resulting noise correlation function is given by:

$$\begin{aligned} c_{\mathsf{z}}[m,l] &= \sum_{k=0}^{L_{\mathsf{z}}} h_{\mathsf{z}}[k] \cdot \sigma_z^2[m-k] \cdot h_{\mathsf{z}}[l+k] \\ &= h_{\mathsf{z}}[0] \cdot \sigma_z^2[m] \cdot h_{\mathsf{z}}[l] \\ &\quad + h_{\mathsf{z}}[1] \cdot \sigma_z^2[m-1] \cdot h_{\mathsf{z}}[l+1] \\ &\quad + h_{\mathsf{z}}[2] \cdot \sigma_z^2[m-2] \cdot h_{\mathsf{z}}[l+2] \\ &= 0.6 \cdot \sigma_z^2[m] \cdot h_{\mathsf{z}}[l] \\ &\quad + 0.4 \cdot \sigma_z^2[m-1] \cdot h_{\mathsf{z}}[l+1] \\ &\quad + 0.2 \cdot \sigma_z^2[m-2] \cdot h_{\mathsf{z}}[l+2], \quad m, l \in \mathcal{Z}. \end{aligned}$$

The memory of the channel is $L_{\mathsf{ch}} = \max\{L_{\mathsf{z}}, L_{\mathsf{h}}\} = 2$ and the period of the channel, denoted with N, is the LCM of the discrete periods P_{h} and P_{z} that satisfies $N > L_{\mathsf{ch}}$, and is set to $N = 8$. For the purpose of this simulation study, the *SNR* is defined as:

$$SNR = \frac{\sigma_s^2 \cdot \mathrm{Tr}\left\{ \left(\mathbb{A}_{L_{\mathsf{tot}},0}[n]\right)^H \cdot \mathbb{A}_{L_{\mathsf{tot}},0}[n] \right\}}{\mathrm{Tr}\left\{ \mathbb{E}\left\{ \mathbf{z}_{L_{\mathsf{tot}},0}[n] \cdot \left(\mathbf{z}_{L_{\mathsf{tot}},0}[n]\right)^H \right\} \right\}}. \quad (35)$$

A detailed derivation of the *SNR* expression in Eq. (35) is presented in [29, Appendix E]. Note that the *SNR* expression in (34) is a special case of the *SNR* expression of Eq. (35).

Synchronization Sequence and Equalizer Parameters:

For both scenarios, the parameters defining the structure of the transmitted frame, corresponding to Fig. 4, are: $N = 8$, $M = 2$, $L_{\mathsf{tot}} = MN = 16$, and $L_{\mathsf{sw}} = MK = 12$. The parameters for the channel estimation and the channel equalizer described in Section VI-A are: $\gamma_{\mathsf{s}}^2 = 1$, $L_{\mathsf{EQ}} = 300$, $e_{\mathrm{r}_0} = 3$, $e_{\mathrm{r}_1} = 2$, and accordingly $|Q_0| = 8649$ and $|Q_1| = 16$. For Scenario 1 we set $J = 300$, $\Omega = 4$, and for Scenario 2 we set $J = 150$, $\Omega = 2$.

Identifying the Optimal Synchronization Sequence:

We first carried out a simulation study for identifying the synchronization sequence that results in the best performance for the SALRT algorithm, that is, finding the synchronization sequence with the largest AUC for the SALRT ROC, at $SNR = -5$ [dB]. To that aim we evaluated the ROC for each synchronization sequence within the set of $|\mathcal{S}|^{L_{\mathsf{sw}}} = 2^{12} = 4096$ different synchronization sequences. The synchronization sequence with the largest AUC of the SALRT ROC for Scenario 1 was identified as:

$$\mathbf{f}_{\mathsf{sw}_1}^T = [-1, 1, -1, 1, -1, 1, 1, -1, 1, -1, 1, -1]\,,$$

while for Scenario 2 the largest AUC is obtained with:

$$\mathbf{f}_{\mathsf{sw}_2}^T = [1, 1, 1, 1, 1, 1, 1, 1, 1, 1, 1, 1]\,.$$

We observe that in the presence of CIR memory and noise correlation, the optimal SW does not have the property of low correlation. This indeed demonstrates that when the channel has memory and/or the noise is correlated, new approaches,

different from the correlator, need to be applied to achieve high detection performance.

The ROC curves for the best synchronization sequence for Scenario 1 are depicted in Figs. 5a, 5b, 5c, and for Scenario 2 in Figs. 6a, 6b, 6c. For each scenario, the ROC curves were obtained with 200000 Monte Carlo simulations for each ROC point, at $SNR = -5$ [dB], $SNR = 0$ [dB], and $SNR = 5$ [dB]. The PDF and the CDF for the AUC of the SALRT ROC, computed over all possible synchronization sequences, are presented in Fig. 7 for Scenario 1 and in Fig. 8 for the Scenario 2. The evaluation of the PDF and of the CDF of the AUC was carried out at $SNR = -5$ [dB], where for each SW, the AUC value was obtained by numerically integrating over the ROC, which was evaluated by averaging over 3000 Monte-Carlo simulations for each point in the ROC.

A. PERFORMANCE EVALUATION

Simulation results for Scenarios 1 and 2 are depicted in Figs. 5a, 5b, 5c, and Figs. 6a, 6b, 6c, respectively. In each figure we also include that ROC for the correlator evaluated with the Zadoff-Chu sequence with parameters $k = 11$ and $L = 12$, see [43, Eq. (2.22)], to demonstrate the impact of the low-correlation property on performance. This Zadoff-Chu sequence is referred to in the following as 'ZC(11)'. We observe that the performance of the ALRT is close to that of the optimal LRT detector in both scenarios for $SNR = 0$ [dB] and $SNR = 5$ [dB]. However, at the lowest SNR, of -5 [dB], the suboptimality of the ALRT becomes evident implying that the log-sum approximation if not useful at that values. The performance of the ALRT and of the RALRT detectors (when the channel is known) are practically indistinguishable, although the RALRT has a smaller computational complexity. The SALRT has better performance than the correlator detector, and, as expected, worse performance than the ALRT and RALRT detectors. It is noted that an advantage of the SALRT and the RALRT detectors over the LRT and the ALRT detectors is their facilitating a controlled trade-off between computational complexity and performance via selection of the search grid sizes, a property that does not exist in the ALRT and the LRT detectors. Recall also that the ALRT and the RALRT detectors *require knowledge of the channel coefficients*, while the SALRT detector does not, which further highlights the advantage of SALRT over the LRT, the ARLT, and the RALRT detectors. We also observe that the correlator with the ZC(11) sequence is considerably inferior to the SALRT with the optimal SW and also considerably inferior to the correlator with the optimal SW. This clearly indicates that low-correlation sequences are not good synchronization sequences when the CIR has memory and/or the noise is correlated.

The computational complexities for the parameters used in Scenario 1 and in Scenario 2 are summarized in Table 2 (see Sections IV-C, V-C, and VI-C for the analysis).

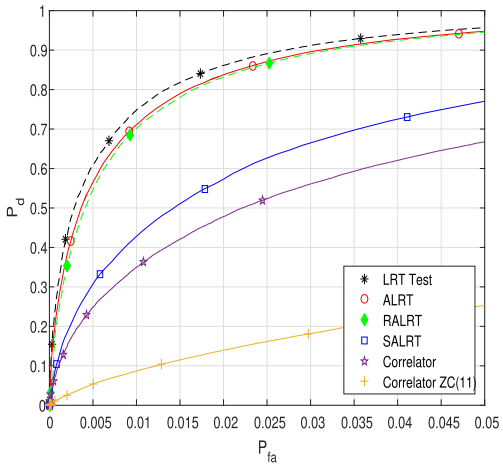

(a) Scenario 1, $SNR = -5$ [dB]

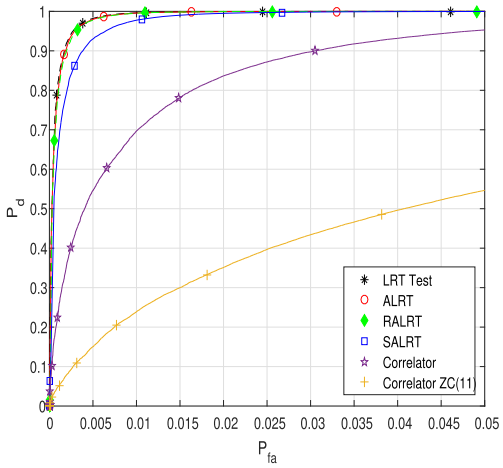

(b) Scenario 1, $SNR = 0$ [dB]

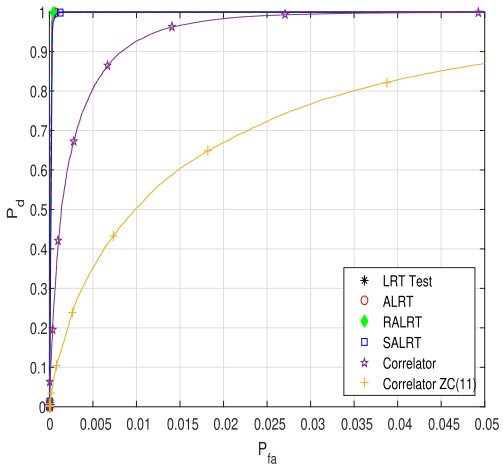

(c) Scenario 1, $SNR = 5$ [dB]

FIGURE 5. ROC performance for the different detectors: LRT with channel knowledge, ALRT with channel knowledge, RALRT with channel knowledge, SALRT without channel knowledge, and correlator without channel knowledge, for Scenario 1 at *SNRs* $= -5, 0, 5$ [dB], for the optimal synchronization sequence $\mathbf{f}^T_{\mathbf{sw}_1} = [-1, 1, -1, 1, -1, 1, 1, -1, 1, -1, 1, -1]$. The ROC for the correlator with the ZC(11) sequence and without channel knowledge is also included.

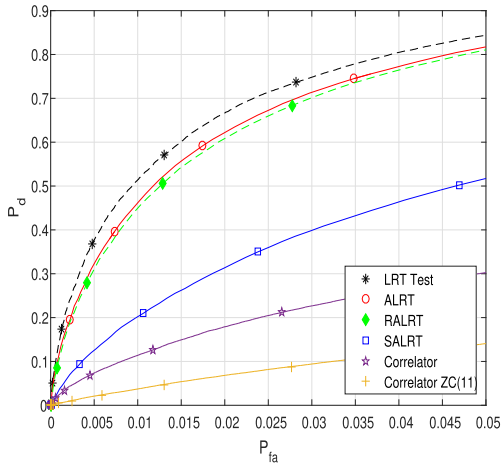

(a) Scenario 2, $SNR = -5$ [dB]

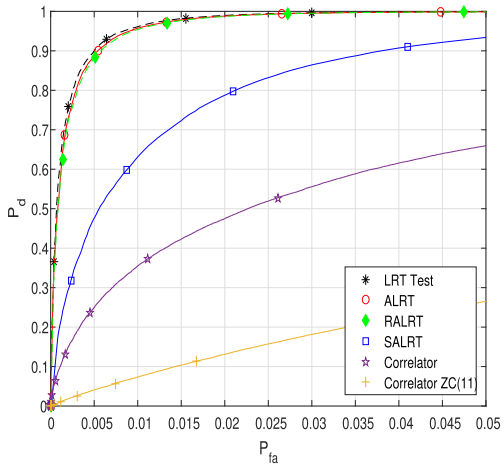

(b) Scenario 2, $SNR = 0$ [dB]

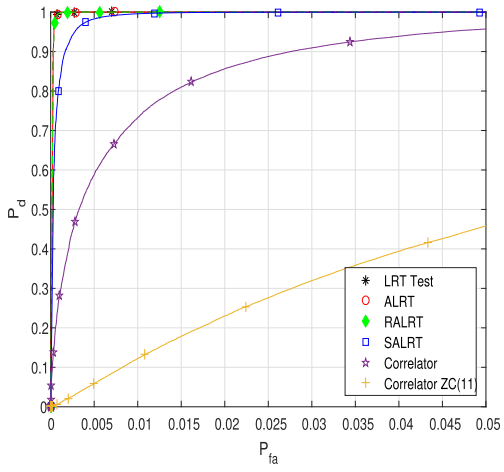

(c) Scenario 2, $SNR = 5$ [dB]

FIGURE 6. ROC performance for the different detectors: LRT with channel knowledge, ALRT with channel knowledge, RALRT with channel knowledge, SALRT without channel knowledge, and correlator without channel knowledge, for Scenario 2 at $SNRs = -5, 0, 5$ [dB], for the optimal synchronization sequence $\mathbf{f}_{sw_2}^T = [1, 1, 1, 1, 1, 1, 1, 1, 1, 1, 1, 1, 1]$. The ROC for the correlator with the ZC(11) sequence and without channel knowledge is also included.

TABLE 2. The computational complexity of the different detectors for Scenario 1 and Scenario 2.

Scenario	Detector	CM $[10^6]$	CA $[10^6]$
1	LRT	11.8	10.9
	ALRT	7.15	6.16
	RALRT	0.94	0.81
	Correlator	$1.3 \cdot 10^{-5}$	$1.1 \cdot 10^{-5}$
	SALRT*	5.38	4.77
2	LRT	11.8	10.9
	ALRT	7.15	6.16
	RALRT	0.94	0.81
	Correlator	$1.3 \cdot 10^{-5}$	$1.1 \cdot 10^{-5}$
	SALRT*	5.38	4.77

$(*)$ For the BPSK constellation set, $c_1 = 1$ and $c_2 = 1$.

Observe that for both scenarios the the number of CMs and of CAs are essentially the same (the least significant digits differ between the values for both scenarios - which is not shown in the table). This is because the dimensions of the operations are mostly affected by the memory of the channel, which is the same in both scenarios. For the LRT (known CIR), the CM is approximately $11.8 \cdot 10^6$, for the ALRT (known CIR) we achieve a relatively small decrease in CM complexity to approximately $7.15 \cdot 10^6$, yet for the RALRT (known CIR) CM complexity is significantly reduced to approximately 10^6. When the CIR is unknown, the applicable detector is the SALRT, whose CM complexity is approximately $5.4 \cdot 10^6$. The correlator has a very small complexity however its performance are considerably inferior to that of the SALRT in both scenarios. Comparing the SALRT and the RALRT we observe that the computational complexity cost for handling an unknown CIR is an increase by approximately 5 times in the computational complexity, but it is still half the complexity of the LRT. In our opinion the SALRT constitutes a good approach for achieving a tradeoff between performance and complexity in FS.

The AUC of the SALRT ROC for the best synchronization sequence in Fig. 5a and Fig. 6a for Scenario 1 and Scenario 2 are 0.9608 and 0.9286, respectively, and the corresponding AUCs for the worst synchronization sequence are 0.8880 and 0.8258, respectively. Based on the CDFs depicted in Figs. 7b and 8b, we can propose a simple procedure for identifying a nearly optimal synchronization sequence without testing all possible synchronization sequences with different CIRs: To that aim, first randomly select 100 synchronization sequences, and evaluate the SALRT ROC and the corresponding AUC for each of these sequences. Then, choose the synchronization sequence with the largest AUC as the (nearly) optimal sequence. From the CDF depicted in Fig. 7b and in Fig. 8b for Scenarios 1 and 2, respectively,

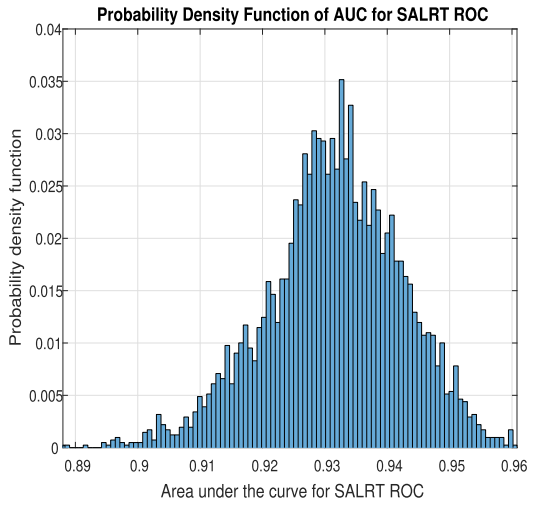

(a) Probability Density Function

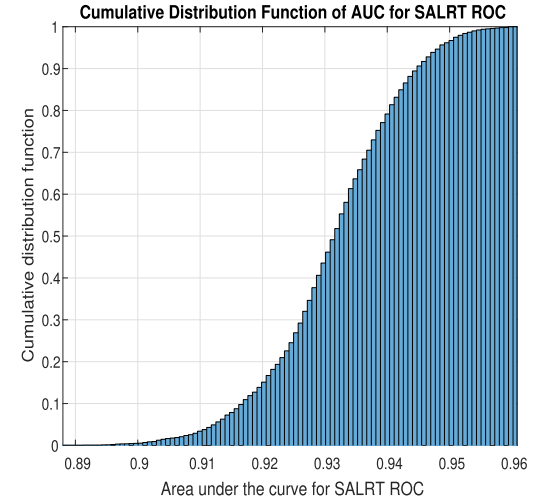

(b) Cumulative Distribution Function

FIGURE 7. Probability density function (a) and cumulative distribution function (b) of the AUC for the SALRT ROC for Scenario 1 for all possible synchronization sequences at $SNR = -5$ [dB].

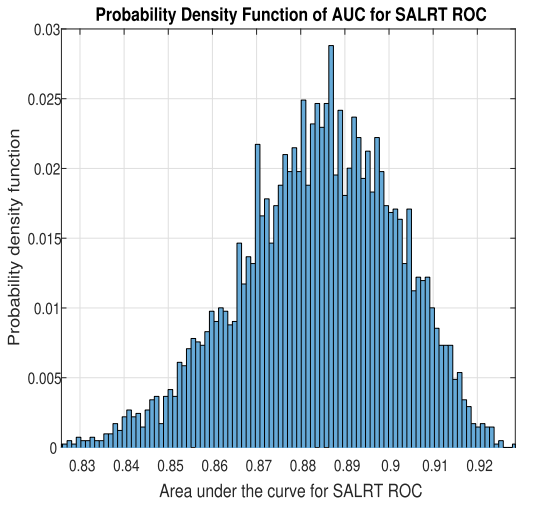

(a) Probability Density Function

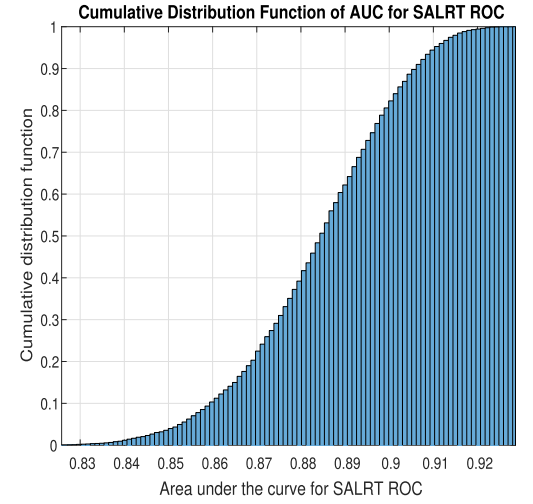

(b) Cumulative Distribution Function

FIGURE 8. Probability density function (a) and cumulative distribution function (b) of the AUC for the SALRT ROC for Scenario 2 for all possible synchronization sequences at $SNR = -5$ [dB].

we note that the range of the AUC whose probability is above 0.9 is $0.945 < \text{AUC}_1 < 0.9608$ and $0.9065 < \text{AUC}_2 < 0.9286$ respectively. The overall range of the AUC values for scenarios 1 and 2 are $0.880 < \text{AUC}_1 < 0.9608$ and $0.8258 < \text{AUC}_2 < 0.9286$, respectively. It follows that the percentage of AUC values with probability higher than 90% for Scenario 1 is $\frac{0.9608-0.945}{0.9608-0.8880} = 21.7\%$, and for Scenario 2 it is $\frac{0.9286-0.9065}{0.9286-0.8258} = 21.5\%$, out of the overall range of the AUC values. Thus, for 100 randomly selected synchronization sequences, approximately 10 sequences will have an AUC higher than 0.945 and 0.9065, for Scenario 1 and 2, respectively. It is noted that 100 sequences is a relatively small fraction of the set of all the possible synchronization sequences e.g., for the example scenarios considered in the simulations using a BPSK constellation with a synchronization sequence whose length is $L_{\text{sw}} = 12$, there are 4096 different possible synchronization sequences.

VIII. CONCLUSIONS

In this paper we studied frame synchronization for LPTV channels with ACGN, where the CIR coefficients are assumed deterministic and unknown. We derived frame synchronization algorithms which account for the channel memory, as previously proposed LRT-based detectors did not account for channel memory, due to the associated computational complexity, see [14], [20]–[23]. Prior works which proposed FS algorithms accounting for channel memory, were based either on ad-hoc considerations, such as the correlator, or on ML criterion [18], hence did not facilitate a tradeoff between the probability of successful detection, p_{d}, and the probability of false alarm, p_{fa}, generally resulting in suboptimal algorithms. We first proposed an ALRT detector, which was shown in the simulations to achieve performance which is very close to that of the optimal LRT detector. We then proposed a new approximate LRT detector which further

reduces the computational complexity by a significant ratio at the cost of an additional decrease in optimally w.r.t. the LRT, referred to as the RALRT. As all above algorithms use knowledge of the channel coefficients in computing the test metric, yet such knowledge is typically not available at the frame synchronization stage, we propose a new blind algorithm, referred to as the SALRT, which handles the lack of CIR knowledge via a non-data-aided iterative CIR estimation. We note that while the SALRT algorithm does not need apriori knowledge of the channel coefficients, it achieves better performance than the correlation detector while in terms of the computational complexity it has a lower computational complexity than the LRT and the ALRT detectors, but a higher computational complexity than the RALRT and the correlator detectors.

APPENDIX

A. DERIVATION OF THE CORRELATION MATRIX FOR HYPOTHESIS H_0

W show that the autocorrelation matrix for $\tilde{\mathbf{R}}_{N,0}[n]$ subject to the H_0 hypothesis, denoted $\mathbb{R}_{\tilde{\mathbf{R}}_{N,0}|H_0}[n,l] \triangleq \mathbb{E}\left\{\tilde{\mathbf{R}}_{N,0}[n+l]\cdot\left(\tilde{\mathbf{R}}_{N,0}[n]\right)^H|H_0\right\}$, is a function only of l, and is independent of n. Applying the statistics of the source sequence together with the periodicity of the noise and the CIR, we obtain that the $\big((a_1+1),(a_2+1)\big)$ element of the correlation matrix is given by:

$$\begin{aligned}
&\mathbb{E}\left\{R[(n+l)\cdot N-a_1]\cdot\left(R\big[n\cdot N-a_2\big]\right)^*\middle|H_0\right\}\\
&=\sum_{l_1=0}^{L_{\mathsf{ch}}}\sum_{l_2=0}^{L_{\mathsf{ch}}}h\big[(n+l)\cdot N-a_1,l_1\big]\cdot h\big[n\cdot N-a_2,l_2\big]\\
&\quad\cdot\mathbb{E}\left\{S\big[(n+l)\cdot N-a_1-l_1\big]\cdot\left(S\big[n\cdot N-a_2-l_2\big]\right)^*\middle|H_0\right\}\\
&\quad+\mathbb{E}\left\{Z\big[(n+l)\cdot N-a_1\big]\cdot\left(Z\big[n\cdot N-a_2\big]\right)^*\middle|H_0\right\}\\
&\overset{(a)}{=}\sum_{l_1=0}^{L_{\mathsf{ch}}}\sum_{l_2=0}^{L_{\mathsf{ch}}}h[-a_1,l_1]\cdot\big(h[-a_2,l_2]\big)^*\cdot\sigma_s^2\\
&\qquad\qquad\cdot\delta[l\cdot N-a_1-l_1+a_2+l_2]\\
&\quad+c_{\mathbf{z}}[-a_2,l\cdot N+a_2-a_1]\,,\\
&\qquad a_1,a_2\in\{0,1,\ldots,K-1\},
\end{aligned}\tag{36}$$

where (a) follows since $N = k_1P_{\mathsf{h}}$, thus $h[n,l_1] = h[n+k_1P_{\mathsf{h}},l_1] = h[n+N,l_1]$, and from the symbol and noise statistics defined in Eqs. (2b) and (1b). From (36) it directly follows that the elements of the correlation matrix $\mathbb{R}_{\tilde{\mathbf{R}}_{N,0}|H_0}[n,l]$ are independent of n, hence, we can write $\mathbb{E}\{\tilde{\mathbf{R}}_{N,0}[n+l](\tilde{\mathbf{R}}_{N,0}[n])^H|H_0\} = \mathbb{R}_{\tilde{\mathbf{R}}_{N,0}|H_0}[l]$, $l\in\mathcal{Z}$. To complete the proof, we must show that the pseudo-autocorrelation matrix for $\tilde{\mathbf{R}}_{N,0}[n]$ subject to the H_0 hypothesis, denoted $\tilde{\mathbb{R}}_{\tilde{\mathbf{R}}_{N,0}|H_0}[n,l] \triangleq \mathbb{E}\{\tilde{\mathbf{R}}_{N,0}[n+l]\cdot(\tilde{\mathbf{R}}_{N,0}[n])^T|H_0\}$ is also a function only of l, and is independent of n. Following parallel arguments of those leading to (36), the $\big((a_1+1),(a_2+1)\big)$ element in the pseudo-autocorrelation matrix $\tilde{\mathbb{R}}_{\tilde{\mathbf{R}}_{N,0}|H_0}[n,l]$, $a_1,a_2\in\{0,1,\ldots,K-1\}$, can be stated as:

$$\begin{aligned}
&\mathbb{E}\left\{R\big[(n+l)\cdot N-a_1\big]\cdot R\big[n\cdot N-a_2\big]\middle|H_0\right\}\\
&\overset{(a)}{=}\sum_{l_1=0}^{L_{\mathsf{ch}}}\sum_{l_2=0}^{L_{\mathsf{ch}}}h[-a_1,l_1]\cdot h[-a_2,l_2]\\
&\quad\cdot\tilde{\sigma}_{\mathbf{s}}^2\cdot\delta[l\cdot N-a_1-l_1+a_2+l_2]\,,
\end{aligned}\tag{37}$$

where (a) uses the fact that from Eq. (2c), $\mathbb{E}\{S[m_1]\cdot S[m_2]\} = \tilde{\sigma}_{\mathbf{s}}^2\cdot\delta[m_1-m_2]$, $\tilde{\sigma}_{\mathbf{s}}^2\in\mathcal{C}$, $\forall\, m_1,m_2\in\mathcal{Z}$, and the fact that because $Z[n]$ is proper complex, its pseudo-autocorrelation function $\tilde{c}_{\mathbf{z}}[m,l] = \mathbb{E}\{Z[m]\cdot Z[m+l]\} = 0$, $\forall m,l\in\mathcal{Z}$, see [29, Section IV-A]. From (37) it directly follows that the elements of the pseudo-autocorrelation matrix $\tilde{\mathbb{R}}_{\tilde{\mathbf{R}}_{N,0}|H_0}[n,l]$ are independent of n, and combined with $\mathbb{E}\{\tilde{\mathbf{R}}_{N,0}[n]|H_0\} = \mathbf{0}$, and with (36), it follows that when H_0 is valid then $\tilde{\mathbf{R}}_{N,0}[n]$ is a WSS random process. Next, we define the mathematical notation $c_{a_1,a_2} \triangleq c_{\mathbf{z}}[-a_2,a_2-a_1]$. We recall that since N is the period of the correlation function then for $l=0$, $c_{\mathbf{z}}[-a_2,l\cdot N+a_2-a_1] = c_{\mathbf{z}}[-a_2,a_2-a_1] = c_{\mathbf{z}}[N-a_2,a_2-a_1] = c_{a_1-N,a_2-N}$, $a_1,a_2\in\mathcal{Z}$. Accordingly, from (1c) it follows that $c_{a_1,a_2} = 0$ for all $|a_1-a_2|>L_{\mathbf{z}}$. It is also noted that after the post-processing $\mathsf{P}\{\cdot\}$, $\tilde{\mathbf{R}}_{N,0}[n\cdot M-m]$ subject to the H_0 hypothesis is a function of mutually independent and identically distributed random vectors, $\mathbf{G}^{(m)}_{L_{\mathsf{tot}},0}[n]$ and $\tilde{\mathbf{Z}}_{N,0}[n\cdot M-m]$ as expressed in Eq. (12), hence, $\tilde{\mathbf{R}}_{N,0}[n\cdot M-m]$ with $m\in\mathcal{M}\triangleq\{0,1,\ldots,M-1\}$ are mutually independent and identically distributed random vectors w.r.t n and m. Next, we define the noise correlation matrix $\mathbb{C}_{\mathbf{z}}\in\mathcal{R}^{K\times K}$ as:

$$[\mathbb{C}_{\mathbf{z}}]_{a_1+1,a_2+1} = c_{a_1,a_2}\tag{38}$$

and prove that the covariance of $\tilde{\mathbf{R}}_{N,0}[n\cdot M-m]$, $m=0,1,\ldots,M-1$, subject to the H_0 hypothesis and given $\mathbf{g}^{(m)}_{L_{\mathsf{tot}},0}[n]$, is equal to $\mathbb{C}_{\mathbf{z}}$, that is:

$$\begin{aligned}
&\mathbb{C}_{\tilde{\mathbf{R}}_{N,0}[n\cdot M-m]|\mathbf{g}^{(m)}_{L_{\mathsf{tot}},0}[n],H_0}\\
&\triangleq\mathbb{E}\left\{\tilde{\mathbf{R}}_{N,0}[n\cdot M-m]\cdot\left(\tilde{\mathbf{R}}_{N,0}[n\cdot M-m]\right)^H\middle|\mathbf{g}^{(m)}_{L_{\mathsf{tot}},0}[n],H_0\right\}\\
&\quad-\mathbb{E}\left\{\tilde{\mathbf{R}}_{N,0}[n\cdot M-m]\middle|\mathbf{g}^{(m)}_{L_{\mathsf{tot}},0}[n],H_0\right\}\\
&\qquad\cdot\mathbb{E}\left\{\left(\tilde{\mathbf{R}}_{N,0}[n\cdot M-m]\right)^H\middle|\mathbf{g}^{(m)}_{L_{\mathsf{tot}},0}[n],H_0\right\}\\
&=\mathbb{C}_{\mathbf{z}}.
\end{aligned}$$

To that aim, first examine $\mathbb{E}\left\{\tilde{\mathbf{R}}_{N,0}[n\cdot M-m]\middle|\mathbf{g}^{(m)}_{L_{\mathsf{tot}},0}[n],H_0\right\}$: From periodicity of the channel, $h[n,l] = h[n+k_1P_{\mathsf{h}},l] = h[n+N,l]$, the relationship $NM = L_{\mathsf{tot}}$, and the fact that $\mathbb{E}\{Z[n]|\mathbf{g}^{(m)}_{L_{\mathsf{tot}},0}[n],H_0\} = 0$, $\forall n\in\mathcal{Z}$, it directly follows that:

$$\mathbb{E}\left\{\tilde{\mathbf{R}}_{N,0}[n\cdot M-m]\middle|\mathbf{g}^{(m)}_{L_{\mathsf{tot}},0}[n],H_0\right\} = \mathbb{B}[n]\cdot\mathbf{g}^{(m)}_{L_{\mathsf{tot}},0}[n]\tag{39}$$

Using (39) we can express

$$\begin{aligned}&\mathbb{E}\Big\{\tilde{\mathbf{R}}_{N,0}[n\cdot M-m]\Big|\mathbf{g}^{(m)}_{L_{\mathsf{tot}},0}[n],H_0\Big\}\\&\quad\cdot\mathbb{E}\Big\{\big(\tilde{\mathbf{R}}_{N,0}[n\cdot M-m]\big)^H\Big|\mathbf{g}^{(m)}_{L_{\mathsf{tot}},0}[n],H_0\Big\}\\&=\mathbb{B}[n]\cdot\mathbf{g}^{(m)}_{L_{\mathsf{tot}},0}[n]\cdot\big(\mathbf{g}^{(m)}_{L_{\mathsf{tot}},0}[n]\big)^H\cdot\big(\mathbb{B}[n]\big)^H\\&\triangleq\mathbb{V}[n,m]\,,\end{aligned}$$

where the elements of matrix $\mathbb{V}[n,m]$ at the (a_1+1)'th row and (a_2+1)'th column, where $a_1,a_2\in\{0,1,\ldots,K-1\}$ are given by:

$$\begin{aligned}&\big[\mathbb{V}[n,m]\big]_{a_1+1,a_2+1}\\&=\sum_{l_1=0}^{L_{\mathsf{ch}}}\sum_{l_2=0}^{L_{\mathsf{ch}}}h[-a_1,l_1]\cdot\big(h[-a_2,l_2]\big)^*\\&\quad\cdot s[nL_{\mathsf{tot}}-mN-a_1-l_1]\cdot\Big(s[nL_{\mathsf{tot}}-mN-a_2-l_2]\Big)^*.\end{aligned}\tag{40}$$

From the definition of $\tilde{\mathbf{R}}_{N,0}[n]$ it immediately follows that the element of the matrix $\mathbb{U}[n,m]\triangleq\mathbb{E}\Big\{\tilde{\mathbf{R}}_{N,0}[n\cdot M-m]\cdot\Big(\tilde{\mathbf{R}}_{N,0}[n\cdot M-m]\Big)^H\Big|\mathbf{g}^{(m)}_{L_{\mathsf{tot}},0}[n],H_0\Big\}$, at the (a_1+1)'th row, and (a_2+1)'th column, $a_1,a_2\in\{0,1,\ldots,K-1\}$, is:

$$\begin{aligned}&\big[\mathbb{U}[n,m]\big]_{a_1+1,a_2+1}\\&=\sum_{l_1=0}^{L_{\mathsf{ch}}}\sum_{l_2=0}^{L_{\mathsf{ch}}}h[-a_1,l_1]\cdot\big(h[-a_2,l_2]\big)^*\\&\quad\cdot s[nL_{\mathsf{tot}}-mN-a_1-l_1]\cdot\Big(s[nL_{\mathsf{tot}}-mN-a_2-l_2]\Big)^*\\&\quad+c_{\mathbf{z}}[-a_2,a_2-a_1].\end{aligned}\tag{41}$$

Thus, we obtain $\mathbb{C}_{\tilde{\mathbf{R}}_{N,0}[n\cdot M-m]|\mathbf{g}^{(m)}_{L_{\mathsf{tot}},0}[n],H_0}=\mathbb{U}[n,m]-\mathbb{V}[n,m]$, hence, the element at the (a_1+1)'th row and the (a_2+1)'th column of $\mathbb{C}_{\tilde{\mathbf{R}}_{N,0}[n\cdot M-m]|\mathbf{g}^{(m)}_{L_{\mathsf{tot}},0}[n],H_0}$ where $a_1,a_2\in\{0,1,\ldots,K-1\}$ is given by:

$$\begin{aligned}&\Big[\mathbb{C}_{\tilde{\mathbf{R}}_{N,0}[n\cdot M-m]|\mathbf{g}^{(m)}_{L_{\mathsf{tot}},0}[n],H_0}\Big]_{a_1+1,a_2+1}\\&\quad=\big[\mathbb{U}[n,m]\big]_{a_1+1,a_2+1}-\big[\mathbb{V}[n,m]\big]_{a_1+1,a_2+1}\\&\quad=c_{\mathbf{z}}[-a_2,a_2-a_1],\end{aligned}\tag{42}$$

It follows from (42) that:

$$\mathbb{C}_{\tilde{\mathbf{R}}_{N,0}[n\cdot M-m]|\mathbf{g}^{(m)}_{L_{\mathsf{tot}},0}[n],H_0}=\mathbb{C}_{\mathbf{z}}.$$

B. DERIVATION OF THE STATISTICS OF THE RECEIVED SIGNAL AND OF THE CORRELATION MATRIX FOR HYPOTHESIS H_1

1) MUTUAL INDEPENDENCE OF $\mathbf{R}_{N,0}[n\cdot M-m]$ FOR HYPOTHESIS H_1

Begin by writing:

$$\begin{aligned}&\tilde{\mathbf{R}}_{N,0}[n\cdot M-m]\\&\quad=\mathbb{B}[n]\cdot\tilde{\mathbf{G}}^{(m)}_{L_{\mathsf{tot}},0}[n]+\tilde{\mathbf{Z}}_{N,0}[n\cdot M-m]\\&\quad=\mathbb{B}[n]\cdot\begin{pmatrix}\mathbf{t}_{M-1-m}\\\mathbf{D}^{(m)}_{L_{\mathsf{tot}},0}[n]\end{pmatrix}+\tilde{\mathbf{Z}}_{N,0}[n\cdot M-m]\\&\quad=\mathbb{B}[n]\cdot\begin{pmatrix}\mathbf{t}_{M-1-m}\\\mathbb{O}_{L_{\mathsf{ch}}\times1}\end{pmatrix}+\mathbb{B}[n]\cdot\begin{pmatrix}\mathbb{O}_{K\times1}\\\mathbf{D}^{(m)}_{L_{\mathsf{tot}},0}[n]\end{pmatrix}\\&\qquad+\tilde{\mathbf{Z}}_{N,0}[n\cdot M-m]\\&\quad=\mathbf{c}[n,m]+\mathbf{X}[n,m]+\tilde{\mathbf{Z}}_{N,0}[n\cdot M-m],\\&\qquad m=0,1,\ldots,M-1\,,\end{aligned}$$

where $\mathbf{c}[n,m]\triangleq\mathbb{B}[n]\cdot\begin{pmatrix}\mathbf{t}_{M-1-m}\\\mathbb{O}_{L_{\mathsf{ch}}\times1}\end{pmatrix}\in\mathcal{C}^{N\times1}$. For a given pair of values of n and m, since $\mathbb{B}[n]$ is a constant matrix and $\mathbf{t}_{M-1-m}$ is a constant vector, then $\mathbf{c}[n,m]$ is a constant vector. Let $\mathbf{X}[n,m]\triangleq\mathbb{B}[n]\cdot\begin{pmatrix}\mathbb{O}_{K\times1}\\\mathbf{D}^{(m)}_{L_{\mathsf{tot}},0}[n]\end{pmatrix}\in\mathcal{C}^{N\times1}$. From the definition of $\mathbf{D}^{(m)}_{L_{\mathsf{tot}},0}[n]$ and $\tilde{\mathbf{Z}}_{N,0}[n\cdot M-m]$ it follows that these are mutually independent vectors over all values of n and m, and that each vector has independent elements. Thus, the random vectors $\mathbf{P}[n,m]\triangleq\mathbf{X}[n,m]+\tilde{\mathbf{Z}}_{N,0}[n\cdot M-m]$ are mutually independent w.r.t. n and m. Accordingly, since $\tilde{\mathbf{R}}_{N,0}[n\cdot M-m]=\mathbf{P}[n,m]+\mathbf{c}[n,m]$, it follows that the vectors $\tilde{\mathbf{R}}_{N,0}[n\cdot M-m]$, subject to the H_1 hypothesis, are mutually independent w.r.t. n and m, for $m=0,1,\ldots,M-1$.

2) DERIVATION OF THE CORRELATION MATRIX FOR HYPOTHESIS H_1

In this appendix we compute $\mathbb{C}_{\tilde{\mathbf{R}}_{N,0}[\cdot n\cdot M-m]|\tilde{\mathbf{g}}^{(m)}_{L_{\mathsf{tot}},0}[n],H_1}$. Beginning with $\mathbb{E}\Big\{\tilde{\mathbf{R}}_{N,0}[n\cdot M-m]\Big|\tilde{\mathbf{g}}^{(m)}_{L_{\mathsf{tot}},0}[n],H_1\Big\}$, then plugging the definition for $\tilde{\mathbf{S}}^{(\mathsf{SW})}_{L_{\mathsf{tot}},0}[n]$ and applying similar steps to those leading to (39) we obtain that:

$$\begin{aligned}&\Big[\mathbb{E}\Big\{\tilde{\mathbf{R}}_{N,0}[n\cdot M-m]\Big|\tilde{\mathbf{g}}^{(m)}_{L_{\mathsf{tot}},0}[n],H_1\Big\}\Big]_{a_1+1,1}\\&=\sum_{l=0}^{L_{\mathsf{ch}}-a_1}h[-a_1,l]f_{L_{\mathsf{sw}}-1-(l+mK)}\\&\quad+\sum_{l=K-a_1}^{L_{\mathsf{ch}}}h\big[-a_1,l\big]\cdot s\big[nL_{\mathsf{tot}}-mN-a_1-l\big],\\&\quad\forall n\in\mathcal{Z},\ m=0,1,\ldots,M-1,\ a_1=0,1,\ldots,K-1.\end{aligned}\tag{43}$$

Using (43) we can derive the elements of matrix $\tilde{\mathbb{V}}[n.m]\triangleq\mathbb{E}\Big\{\tilde{\mathbf{R}}_{N,0}[n\cdot M-m]\Big|\tilde{\mathbf{g}}^{(m)}_{L_{\mathsf{tot}},0}[n],H_1\Big\}\cdot\mathbb{E}\Big\{\big(\tilde{\mathbf{R}}_{N,0}[n\cdot M-m]\big)^H\Big|\tilde{\mathbf{g}}^{(m)}_{L_{\mathsf{tot}},0}[n],H_1\Big\}$ as follows: Defining the sets $\mathcal{I}_1=\{0,1,\ldots,K-L_{\mathsf{ch}}-1\}$ and $\mathcal{I}_2=\{K-L_{\mathsf{ch}},K-(L_{\mathsf{ch}}-1),\ldots,K-1\}$, we write for $a_1,a_2\in\{0,1,\ldots,K-1\}$:

$$\begin{aligned}&\big[\tilde{\mathbb{V}}[n,m]\big]_{a_1+1,a_2+1}\\&\quad=\mathbb{E}\Big\{R\big[(n\cdot M-m)N-a_1\big]\Big|\tilde{\mathbf{g}}^{(m)}_{L_{\mathsf{tot}},0}[n],H_1\Big\}\\&\qquad\cdot\mathbb{E}\Big\{\Big(R\big[(n\cdot M-m)N-a_2\big]\Big)^*\Big|\tilde{\mathbf{g}}^{(m)}_{L_{\mathsf{tot}},0}[n],H_1\Big\}\end{aligned}$$

and obtain that $\left[\tilde{\mathbb{V}}[n,m]\right]_{a_1+1,a_2+1}$ depend on a_1 and a_2 as follows

$$\begin{aligned}
&\underline{a_1,a_2\in\mathcal{I}_1}\\
&\left[\tilde{\mathbb{V}}[n,m]\right]_{a_1+1,a_2+1}\\
&=\sum_{l_1=0}^{L_{\mathsf{ch}}}\sum_{l_2=0}^{L_{\mathsf{ch}}}h\big[-a_1,l_1\big]\cdot\Big(h\big[-a_2,l_2\big]\Big)^*\\
&\qquad\cdot f_{L_{\mathsf{sw}}-1-(l_1+mK+a_1)}\cdot\Big(f_{L_{\mathsf{sw}}-1-(l_2+mK+a_2)}\Big)^*\\
&\underline{a_1\in\mathcal{I}_1,\ a_2\in\mathcal{I}_2}\\
&\left[\tilde{\mathbb{V}}[n,m]\right]_{a_1+1,a_2+1}\\
&=\sum_{l_1=0}^{L_{\mathsf{ch}}}\sum_{l_2=0}^{K-1-a_2}h\big[-a_1,l_1\big]\cdot\Big(h\big[-a_2,l_2\big]\Big)^*\\
&\qquad\cdot f_{L_{\mathsf{sw}}-1-(l_1+mK+a_1)}\cdot\Big(f_{L_{\mathsf{sw}}-1-(l_2+mK+a_2)}\Big)^*\\
&\quad+\sum_{l_1=0}^{L_{\mathsf{ch}}}\sum_{l_2=K-a_2}^{L_{\mathsf{ch}}}h\big[-a_1,l_1\big]\cdot\Big(h\big[-a_2,l_2\big]\Big)^*\\
&\qquad\cdot f_{L_{\mathsf{sw}}-1-(l_1+mK+a_1)}\cdot\Big(s\big[nL_{\mathsf{tot}}-mN-a_2-l_2)\big]\Big)^*\\
&\underline{a_1\in\mathcal{I}_2,\ a_2\in\mathcal{I}_1}\\
&\left[\tilde{\mathbb{V}}[n,m]\right]_{a_1+1,a_2+1}\\
&=\sum_{l_1=0}^{K-1-a_1}\sum_{l_2=0}^{L_{\mathsf{ch}}}h\big[-a_1,l_1\big]\cdot\Big(h\big[-a_2,l_2\big]\Big)^*\\
&\qquad\cdot f_{L_{\mathsf{sw}}-1-(l_1+mK+a_1)}\cdot\Big(f_{L_{\mathsf{sw}}-1-(l_2+mK+a_2)}\Big)^*\\
&\quad+\sum_{l_1=K-a_1}^{L_{\mathsf{ch}}}\sum_{l_2=0}^{L_{\mathsf{ch}}}h\big[-a_1,l_1\big]\cdot\Big(h\big[-a_2,l_2\big]\Big)^*\\
&\qquad\cdot s\big[nL_{\mathsf{tot}}-mN-a_1-l_1\big]\cdot\Big(f_{L_{\mathsf{sw}}-1-(l_2+mK+a_2)}\Big)^*\\
&\underline{a_1,a_2\in\mathcal{I}_2}\\
&\left[\tilde{\mathbb{V}}[n,m]\right]_{a_1+1,a_2+1}\\
&=\sum_{l_1=0}^{K-1-a_1}\sum_{l_2=0}^{K-1-a_2}h\big[-a_1,l_1\big]\cdot\Big(h\big[-a_2,l_2\big]\Big)^*\\
&\qquad\cdot f_{L_{\mathsf{sw}}-1-(l_1+mK+a_1)}\cdot\Big(f_{L_{\mathsf{sw}}-1-(l_2+mK+a_2)}\Big)^*\\
&\quad+\sum_{l_1=0}^{K-1-a_1}\sum_{l_2=K-a_2}^{L_{\mathsf{ch}}}h\big[-a_1,l_1\big]\cdot\Big(h\big[-a_2,l_2\big]\Big)^*\\
&\qquad\cdot f_{L_{\mathsf{sw}}-1-(l_1+mK+a_1)}\cdot\Big(s\big[nL_{\mathsf{tot}}-mN-a_2-l_2\big]\Big)^*\\
&\quad+\sum_{l_1=0}^{K-1-a_1}\sum_{l_2=K-a_2}^{L_{\mathsf{ch}}}h\big[-a_1,l_1\big]\cdot\Big(h\big[-a_2,l_2\big]\Big)^*\\
&\qquad\cdot f_{L_{\mathsf{sw}}-1-(l_1+mK+a_1)}\cdot\Big(s\big[nL_{\mathsf{tot}}-mN-a_2-l_2\big]\Big)^*\\
&\quad+\sum_{l_1=K-a_1}^{L_{\mathsf{ch}}}\sum_{l_2=K-a_2}^{L_{\mathsf{ch}}}h\big[-a_1,l_1\big]\cdot\Big(h\big[-a_2,l_2\big]\Big)^*\\
&\qquad\cdot s\big[nL_{\mathsf{tot}}-mN-a_1-l_1)\big]\cdot\Big(s\big[nL_{\mathsf{tot}}-mN-a_2-l_2\big]\Big)^*
\end{aligned}\tag{44}$$

Next, we explicitly express the elements of the matrix $\tilde{\mathbb{U}}[n,m]\triangleq\mathbb{E}\Big\{\tilde{\mathbf{R}}_{N,0}[n\cdot M-m]\cdot\big(\tilde{\mathbf{R}}_{N,0}[n\cdot M-m]\big)^H\Big|\tilde{\mathbf{g}}^{(m)}_{L_{\mathsf{tot}},0}[n],H_1\Big\}$, at the (a_1+1)'th row and the (a_2+1)'th column, $a_1,a_2\in\{0,1,\ldots,K-1\}$. Using steps similar to those leading to (44) we obtain:

$$\begin{aligned}
&\left[\tilde{\mathbb{U}}[n,m]\right]_{a_1+1,a_2+1}\\
&\quad=\mathbb{E}\Big\{R\big[(n\cdot M-m)N-a_1\big]\\
&\qquad\cdot\Big(R\big[(n\cdot M-m)N-a_2\big]\Big)^*\Big|\tilde{\mathbf{g}}^{(m)}_{L_{\mathsf{tot}},0}[n],H_1\Big\}\\
&\quad=\left[\tilde{\mathbb{V}}[n,m]\right]_{a_1+1,a_2+1}+c_{\mathbf{z}}\big[-a_2,a_2-a_1\big]
\end{aligned}\tag{45}$$

Noting that $\mathbb{C}_{\tilde{\mathbf{R}}_{N,0}[n\cdot M-m]|\tilde{\mathbf{g}}^{(m)}_{L_{\mathsf{tot}},0}[n],H_0}=\tilde{\mathbb{U}}[n,m]-\tilde{\mathbb{V}}[n,m]$, it follows that the element at the (a_1+1)'th row and the (a_2+1)'th column, where $a_1,a_2\in\{0,1,\ldots,K-1\}$, is given by:

$$\begin{aligned}
&\left[\mathbb{C}_{\tilde{\mathbf{R}}_{N,0}[n\cdot M-m]|\tilde{\mathbf{g}}^{(m)}_{L_{\mathsf{tot}},0}[n],H_1}\right]_{a_1+1,a_2+1}\\
&\quad=\left[\tilde{\mathbb{U}}[n,m]\right]_{a_1+1,a_2+1}-\left[\tilde{\mathbb{V}}[n,m]\right]_{a_1+1,a_2+1}\\
&\quad=c_{\mathbf{z}}\big[-a_2,a_2-a_1\big].
\end{aligned}\tag{46}$$

Hence, $\mathbb{C}_{\tilde{\mathbf{R}}_{N,0}[n\cdot M-m]|\tilde{\mathbf{g}}^{(m)}_{L_{\mathsf{tot}},0}[n],H_1}=\mathbb{C}_{\mathbf{z}}$.

REFERENCES

[1] R. Scholtz, "Frame synchronization techniques," *IEEE Trans. Commun.*, vol. 28, no. 8, pp. 1204–1213, Aug. 1980.

[2] P. Robertson, "Optimal frame synchronization for continuous and packet data transmission," Ph.D. dissertation, Dept. Elect. Eng., Bundeswehr Univ. Munich, Neubiberg, Germany, 1995.

[3] U. Mengali, *Synchronization Techniques for Digital Receivers*. New York, NY, USA: Springer, 2013.

[4] W. A. Gardner, A. Napolitano, and L. Paura, "Cyclostationarity: Half a century of research," *Signal Process.*, vol. 86, no. 4, pp. 639–697, Apr. 2006.

[5] M. Nassar, J. Lin, Y. Mortazavi, A. Dabak, I. Kim, and B. Evans, "Local utility power line communications in the 3–500 kHz band: Channel impairments, noise, and standards," *IEEE Signal Process. Mag.*, vol. 29, no. 5, pp. 116–127, Sep. 2012.

[6] R. Shaked, N. Shlezinger, and R. Dabora, "Joint estimation of carrier frequency offset and channel impulse response for linear periodic channels," *IEEE Trans. Commun.*, vol. 66, no. 1, pp. 302–319, Jan. 2018.

[7] J. G. Andrews, S. Buzzi, W. Choi, S. V. Hanly, A. Lozano, A. C. K. Soong, and J. C. Zhang, "What will 5G be?" *IEEE J. Sel. Areas Commun.*, vol. 32, no. 6, pp. 1065–1082, Jun. 2014.

[8] L. Dai, B. Wang, Y. Yuan, S. Han, C.-L. I, and Z. Wang, "Non-orthogonal multiple access for 5G: Solutions, challenges, opportunities, and future research trends," *IEEE Commun. Mag.*, vol. 53, no. 9, pp. 74–81, Sep. 2015.

[9] X. Hong, Z. Chen, C.-X. Wang, S. A. Vorobyov, and J. S. Thompson, "Cognitive radio networks: Interference cancelation and management techniques," *IEEE Veh. Technol. Mag.*, vol. 4, no. 4, pp. 76–84, Dec. 2009.

[10] J. Campbell, A. Gibbs, and B. Smith, "The cyclostationary nature of crosstalk interference from digital signals in multipair cable—Part I: Fundamentals," *IEEE Trans. Commun.*, vol. 31, no. 5, pp. 629–637, May 1983.

[11] M. A. Mchenry, D. Roberson, and R. J. Matheson, "Phone to fridge: Shut up!" *IEEE Spectr.*, vol. 52, no. 9, pp. 50–56, Sep. 2015.

[12] J. Massey, "Optimum frame synchronization," *IEEE Trans. Commun.*, vol. 20, no. 2, pp. 115–119, Apr. 1972.

[13] B. Ramakrishnan, "Frame synchronization with large carrier frequency offsets: Point estimation versus hypothesis testing," in *Proc. 7th Int. Symp. Commun. Syst., Netw. Digit. Signal Process. (CSNDSP)*, Newcastle upon Tyne, U.K., Jul. 2010, pp. 45–50.
[14] Y. Liang, D. Rajan, and O. E. Eliezer, "Sequential frame synchronization based on hypothesis testing with unknown channel state information," *IEEE Trans. Commun.*, vol. 63, no. 8, pp. 2972–2984, Aug. 2015.
[15] P. Nielsen, "Some optimum and suboptimum frame synchronizers for binary data in Gaussian noise," *IEEE Trans. Commun.*, vol. 21, no. 6, pp. 770–772, Jun. 1973.
[16] G. Lui and H. Tan, "Frame synchronization for Gaussian channels," *IEEE Trans. Commun.*, vol. 35, no. 8, pp. 818–829, Aug. 1987.
[17] Z. Yong Choi and Y. H. Lee, "Frame synchronization in the presence of frequency offset," *IEEE Trans. Commun.*, vol. 50, no. 7, pp. 1062–1065, Jul. 2002.
[18] B. H. Moon and S. Soliman, "ML frame synchronization for the Gaussian channel with ISI," in *Proc. IEEE Int. Conf. Commun. (ICC)*, Denver, CO, USA, Jun. 1991, pp. 1698–1702.
[19] Y. Wang, K. Shi, and E. Serpedin, "Continuous-mode frame synchronization for frequency-selective channels," *IEEE Trans. Veh. Technol.*, vol. 53, no. 3, pp. 865–871, May 2004.
[20] J. A. Gansman, M. P. Fitz, and J. V. Krogmeier, "Optimum and suboptimum frame synchronization for pilot-symbol-assisted modulation," *IEEE Trans. Commun.*, vol. 45, no. 10, pp. 1327–1337, Oct. 1997.
[21] M. Chiani and M. G. Martini, "Optimum synchronization of frames with unknown variable lengths on Gaussian channels," in *Proc. IEEE Global Telecommun. Conf. (GLOBECOM)*, Dallas, TX, USA, vol. 6, Jun. 2004, pp. 4087–4091.
[22] M. Chiani and M. G. Martini, "Practical frame synchronization for data with unknown distribution on AWGN channels," *IEEE Commun. Lett.*, vol. 9, no. 5, pp. 456–458, May 2005.
[23] M. Chiani, "Noncoherent frame synchronization," *IEEE Trans. Commun.*, vol. 58, no. 5, pp. 1536–1545, May 2010.
[24] K. Hasselmann and T. P. Barnett, "Techniques of linear prediction for systems with periodic statistics," *J. Atmos. Sci.*, vol. 38, no. 10, pp. 2275–2283, Oct. 1981.
[25] J. K. Cavers, "An analysis of pilot symbol assisted modulation for Rayleigh fading channels (mobile radio)," *IEEE Trans. Veh. Technol.*, vol. 40, no. 4, pp. 686–693, Nov. 1991.
[26] G. B. Giannakis, "Cyclostationary signal analysis," in *Digital Signal Processing Handbook*, V. K. Madisetti and D. B. Williams, Eds. Boca Raton, FL, USA: CRC Press, 1999, ch. 17.
[27] E. Parzen and M. Pagano, "An approach to modeling seasonally stationary time series," *J. Econometrics*, vol. 9, nos. 1–2, pp. 137–153, Jan. 1979.
[28] H. J. Newton, "Using periodic autoregressions for multiple spectral estimation," *Technometrics*, vol. 24, no. 2, pp. 109–116, May 1982.
[29] O. Kolaman and R. Dabora, "A new frame synchronization algorithm for linear periodic channels with memory—Full version," Jul. 2020, *arXiv:2007.05571v1*. [Online]. Available: https://arxiv.org/abs/2007.05571v1
[30] M. Chiani and M. G. Martini, "On sequential frame synchronization in AWGN channels," *IEEE Trans. Commun.*, vol. 54, no. 2, pp. 339–348, Feb. 2006.
[31] H. L. Van Trees, *Detection, Estimation, Modulation Theory, Part I: Detection, Estimation, Linear Modulation Theory*. Hoboken, NJ, USA: Wiley, 2004.
[32] W. Mendenhall, R. J. Beaver, and B. M. Beaver, *Introduction to Probability and Statistics*. Boston, MA, USA: Cengage Learning, 2012.
[33] F. Nielsen and K. Sun, "Guaranteed bounds on the Kullback-Leibler divergence of univariate mixtures using piecewise log-sum-exp inequalities," 2016, *arXiv:1606.05850*. [Online]. Available: http://arxiv.org/abs/1606.05850
[34] D. Godard, "Self-recovering equalization and carrier tracking in two-dimensional data communication systems," *IEEE Trans. Commun.*, vol. 28, no. 11, pp. 1867–1875, Nov. 1980.
[35] J. G. Proakis and M. Salehi, *Digital Communications*, vol. 4. New York, NY, USA: McGraw-Hill, 2001.
[36] G. Ungerboeck, "Theory on the speed of convergence in adaptive equalizers for digital communication," *IBM J. Res. Develop.*, vol. 16, no. 6, pp. 546–555, Nov. 1972.
[37] S. N. Crozier, D. D. Falconer, and S. A. Mahmoud, "Least sum of squared errors (LSSE) channel estimation," *IEE Proc.—F Radar Signal Process.*, vol. 138, no. 4, pp. 371–378, Aug. 1991.
[38] M. Morelli and U. Mengali, "Carrier-frequency estimation for transmissions over selective channels," *IEEE Trans. Commun.*, vol. 48, no. 9, pp. 1580–1589, Sep. 2000.
[39] S. Houcke, A. Chevreuil, and P. Loubaton, "Blind equalization-case of an unknown symbol period," *IEEE Trans. Signal Process.*, vol. 51, no. 3, pp. 781–793, Mar. 2003.
[40] A. A. Karatsuba, "The complexity of computations," *Proc. Steklov Inst. Math.-Interperiodica Transl.*, vol. 211, pp. 169–183, Jan. 1995.
[41] T. Fawcett, "An introduction to ROC analysis," *Pattern Recognit. Lett.*, vol. 27, no. 8, pp. 861–874, Jun. 2006.
[42] M. Kumar and R. Dabora, "A novel sampling frequency offset estimation algorithm for OFDM systems based on cyclostationary properties," *IEEE Access*, vol. 7, pp. 100692–100705, 2019.
[43] K. Fazel and S. Kaiser, *Multi-Carrier Spread Spectr. Systems: From OFDM MC-CDMA to LTE WiMAX*, 2nd ed. Hoboken, NJ, USA: Wiley, 2008.

OREN KOLAMAN (Student Member, IEEE) received the B.Sc. degree in electrical and computer engineering from the Ben-Gurion University of the Negev, Israel, in 2016, where he is currently pursuing the M.Sc. degree in electrical and computer engineering. His research interests include signal processing for communications and frame synchronization.

RON DABORA (Senior Member, IEEE) received the B.Sc. and M.Sc. degrees from Tel Aviv University, in 1994 and 2000, respectively, and the Ph.D. degree from Cornell University, USA, in 2007, all in electrical engineering. From 1994 to 2000, he was with the Ministry of Defense, Israel, and from 2000 to 2003, he was with the Algorithms Group, Millimetrix Broadband Networks, Israel. From 2007 to 2009, he was a Postdoctoral Researcher with the Department of Electrical Engineering, Stanford University, USA. Since 2009, he has been with the Department of Electrical and Computer Engineering, Ben-Gurion University of the Negev, Israel, where he is currently an Associate Professor. His research interests include network information theory, wireless communications, and power line communications. He has served as a TPC Member in a number of international conferences, including WCNC, PIMRC, and ICC. From 2012 to 2014, he has served as an Associate Editor for the IEEE SIGNAL PROCESSING LETTERS. From 2014 to 2019, he has served as a Senior Area Editor for the IEEE SIGNAL PROCESSING LETTERS.